UNIVERSITEIT VAN PRETORIA
UNIVERSITY OF PRETORIA
YUNIBESITHI YA PRETORIA

Investigation of vasculogenic mimicry in melanoma tissue

Dissertation submitted in partial fulfilment in accordance with the requirements for the degree,

Master of Science (Human Physiology)

Department of Physiology

School of Medicine

Faculty of Health Sciences

University of Pretoria

Candidate	Supervisor	Co - supervisor
Rakolote Bruce Matlala	Prof. P. Mabeta	Dr. B. Flepisi
Student number: 10199544	Department of Physiology	Department of Pharmacology
Department of Physiology	Faculty of Health Sciences	Faculty of Health Sciences
Faculty of Health Sciences	University of Pretoria	University of Pretoria
University of Pretoria		

Co-supervisor	Head of Department
Prof. M. Bida	Prof. A. Joubert
Department of Anatomical Pathology	Department of Physiology
Faculty of Health Sciences	Faculty of Health Sciences
University of Pretoria	University of Pretoria

January 2025

Declaration

I, Rakolote Bruce Matlala, student number 10199544 hereby declare that this dissertation, "*Investigation of vasculogenic mimicry in melanoma tissue,*" is submitted in accordance with the requirements for the Master of Science in Human Physiology degree at the University of Pretoria, is my own original work and has not previously been submitted to any other institution of higher learning. All sources cited or quoted in this research work are indicated and acknowledged with a comprehensive list of references.

.....

Rakolote Bruce Matlala

14 January 2025

Dedication

I dedicate this research to these people very dear to my heart:

My dearest Mom, Modipadi a Mphele

My Father, Hlabirwa a Phaahla

My brothers, Lethamaga, Lekgotla, Matlaweng and Mantinyane

Acknowledgements

To have achieved this milestone in my life, I would like to express my sincere gratitude to the following people and institutions:

- Great God Almighty, who provided me the strength, courage, wisdom and perseverance to complete this study.
- Professor Peace Mabeta (lead supervisor) firstly for granting me an opportunity to be part of this research, for her invaluable advice, guidance and inspiring motivation during difficult times during the research.
- Professor Meshack Bida (co-supervisor) for his exceptional guidance and support in conducting immunohistochemistry experiments. His invaluable contributions to review stained slides have been instrumental to this work.
- Dr Brian Flepisi (co-supervisor) for his guidance and support in conducting western blot experiments, not forgetting the comments during protocol design and final dissertation write-up to improve on the quality of the work.
- University of Pretoria for granting me the Postgraduate Bursary which removed financial stress while working on this research.
- Southern Ear, Nose and Throat (PTY) Ltd for also providing funding assistance for 2 years to enable completion of this degree, I am truly grateful.
- My mom (Queen of my heart), dad, siblings, sister-in-law and niece thank you for always believing in me, even when I doubt myself. Thank you Modipadi for the words of wisdom, encouragement, motivation, being my confidant and cheerleader in all that I do in this life. As well as the early morning prayers when I wanted to give up & continuous encouragement to offer my work and studies to God Almighty.
- My laboratory mates, especially Lebogang Matutule, words are not enough to express my gratitude for your unwavering support to “master” most of the critical techniques required for progress with experiments.
- Vuledzani Takalani for her assistance in conducting immunohistochemistry experiments from sample preparation and validation of proteins of interest. Your support and guidance on how to successfully complete this objective has been truly helpful, Thank you.

- Abuti Paulos and Malome Lucky, for taking the time to assist retrieve melanoma patient blocks for immunohistochemistry study, thank you so much for the support and having to go the extra mile during your free time to get the samples timeously.
- My friends and colleagues for their motivation and push when it seemed impossible.
- Mrs Anne T. McCoy, my mentor and life-coach, your words of encouragement and advise will never go unnoticed especially by those around me. You inspire me in many ways “my words” cannot describe. Thank you very much for the support.

“I believe in God, Even When He Is Silent”

Executive Summary

Melanoma is an invasive and aggressive form of skin cancer developing from melanocytes in the basal layer of the epidermis. Worldwide, the incidence of melanoma continues to increase, accounting for approximately 80% of all skin cancer-related deaths in 2020. In South Africa, the overall incidence of melanoma is approximately 2.7 per 100,000 people. In comparison, melanoma accounted for a similar proportion of approximately 80% of all skin cancer-related deaths in 2012, with an estimated 55,000 deaths globally. The rapid proliferation of melanocytes increases oxygen and nutrient requirements and results in increased vascularisation as a coping mechanism to meet the metabolic requirements of the tumour. Angiogenesis, the formation of new blood vessels from existing micro-vessels, is an important mechanism of vascularisation in melanoma. Various anti-angiogenic drugs such as bevacizumab have been employed to inhibit blood vessel formation in melanoma. However, resistance develops partly due to alternative pathways of vascularisation, mainly vasculogenic mimicry (VM). Vasculogenic mimicry is the process of forming highly patterned matrix and tubular channels lined with tumour cells, evidently known to conduct fluid movement. The process entails melanoma cell proliferation and their migration, and their subsequent coalescing into vessel-like structures. The formation of VM is regulated by multiple factors including, vascular cell adhesion molecule -1 (VCAM1), vascular endothelial growth factor-A (VEGF-A), and nodal. Therefore, the aim of this study was to investigate the vasculogenic mimicry in melanoma tissue by evaluating cell proliferation, migration, and the expression of molecular regulators of vasculogenic mimicry.

For *in vivo* studies, immunohistochemistry (IHC) was utilised to determine the expression of the proteins VCAM1 and VEGF-A in tissue samples of melanoma patients. As challenges were encountered with optimising western blotting technique, further studies were undertaken using *in vitro* models .

The endothelioma (sEnd.2) and melanoma (B16-F10) cell lines, employed in this study as *in vitro* models for benign and malignant skin tumours, were maintained in an incubator at 37 °C in a humidified atmosphere containing 5% CO_2. Melanoma and endothelioma viability and growth patterns were studied *in vitro* using the crystal violet assay. Furthermore, cell morphology characteristics were studied using polarisation-

optical interference contrast and light microscopy to augment cell growth data. Since vascular endothelial growth factor receptor-1 (VEGFR-1) is known to signal vasculogenic mimicry, western blot was employed to investigate the expression of the key receptor which promotes vasculogenic mimicry, VEGFR-1.

The *in vitro* scratch migration assay and real-time, label-free xCELLigence technologies were used to study the effect of VEGFR-1 blockade on the migration of cells as well as cell invasion and migration respectively.

In vivo studies showed that VCAM1 and VEGF-A in melanoma tissue were positively expressed intratumorally, suggesting their potential involvement in tumour growth and vasculogenic mimicry. This expression may contribute to melanoma progression and survival by promoting the formation of vessel-like structures, thereby facilitating nutrient and oxygen supply to the tumour cells.

The results from *in vitro* studies demonstrated significant attenuation of melanoma cell growth. Morphology study results showed significant changes including cell rounding, membrane blebbing and reduction in cell density, which indicate cytoskeletal disruption and apoptosis. These observations, along with decreased cell density, suggest a reduction in cell proliferation and an increase in cell death, confirming the apoptotic effects of sunitinib malate. Western blot studies revealed that melanoma cells express VEGFR-1. Cell migration plays a critical role in vasculogenic mimicry by allowing tumour cells to create vessel-like structures that mimic blood vessels, promoting tumour growth, invasion, and the bypass of conventional angiogenesis, which in turn aids tumour progression and therapy resistance. In this regard, cell migration studies showed that VEGFR-1 blockade significantly decreased the rate of cell migration and invasion, highlighting the crucial role of VEGFR-1 in these processes and its potential as a therapeutic target. Therefore, taken together, these outcomes further support the evidence for the presence of vasculogenic mimicry in melanoma and thereby provide an opportunity for further investigation on the use of combination therapies to improve patient outcome.

Keywords: Melanoma, vasculogenic mimicry, tumour progression, vascular endothelial growth factor, endothelial cells

Table of Contents

List of Figures

List of Tables

List of abbreviations

AJCC – American Joint Committee for Cancer

ATCC – American type culture collection

BCA – Bicinchoninic acid

BCC – Basal cell carcinoma

bFGF – Basic fibroblast growth factor

BRAF – B-Raf proto-oncogene, serine/threonine kinase

BSA – Bovine serum albumin

BCIP - 5-bromo-4-chloro-3-indolyl phosphate

CD – Cluster differentiation

CDKN2A – Cyclin-dependent kinase inhibitor 2A

CI – Confidence interval

CO_2 – Carbon dioxide

CSC – Cancer stem cell

DMEM – Dulbecco's modified Eagles's medium

DP – Dual plate

DNA – Deoxyribonucleic acid

ECM – Extracellular matrix

ECs – Endothelial cells

EMT – Epithelial-mesenchymal transition

EphA2 – Ephrin type-A receptor 2

ERK – Extracellular signal-regulated kinase

FAK – Focal adhesion kinase

FBS – Fetal bovine serum

FDA – Food and Drug Administration

h - Hours

HIF – Hypoxia inducible factor

HRE – Hypoxia responsive elements

IC_{50} – Inhibitory concentration for 50% of cells

IHC – Immunohistochemistry

Ln-5 – Laminin 5

MAPK – Mitogen-activated protein kinase

MEDS – Melanoma diagnosis system

MEK – Mitogen-activated protein kinase

min – Minute(s)

mL - millilitre

mm – Millimetre

MMP – Matrix metalloproteinase

MT-MMP – Membrane type – matrix metalloproteinase

OS – Odds of survival

PAS – Periodic acid Schiff

PBS – Phosphate buffer solution

PDGF – Platelet derived growth factor

PDT – Photodynamic therapy

PFS – Progression free survival

pH – Potential of Hydrogen

PI3K – Phosphoinositide 3-kinase

PlasDIC – Polarisation-optical interference contrast

rpm – Revolutions per minute

RR – Relative risk

SCC – Squamous cell carcinoma

SDS – Sodium dodecyl

TGF β – Transforming growth factor β

TNM – Tumour, Node, Metastasis

VE-Cad – Vascular endothelial cadherin

VEGF – Vascular endothelial growth factor

VEGFR – Vascular endothelial growth factor receptor

VM – Vasculogenic mimicry

α-MSH – Melanocortin

CHAPTER 1: LITERATURE REVIEW

1.1 Introduction

The skin is the largest organ of the human body, it accounts for 15% of the total adult body weight and occupies a 1.5-2 m^2 surface area[1, 2]. It provides a mechanical barrier against the external environment, regulates temperature and fluid balance, and is also responsible for other metabolic processes[1]. It is a complex epithelial and mesenchymal tissue comprising two main layers: the epidermis and the dermis[3].

1.1.1 The epidermis

The epidermis is the outermost layer of the skin and is responsible for skin colour, texture and moisture[3]. It is composed of 95% keratinocytes and 5% melanocytes, Langerhans cells and Merkel cells[1]. Furthermore, the epidermis is divided into four main layers depending on the state of the keratinocyte maturation from the deep to superficial layer [1, 3]. The deepest layer is the basal layer, composed of basal stem cells which proliferate to form keratinocytes and consequently the other layers superficially as they mature[3].

Melanocytes are dendritic cells derived from the neural crest stem cells through differentiation[1, 4]. The primary function of melanocytes is to synthesise melanin; packaged in subcellular organelles known as melanosomes and then transported to nearby keratinocytes to form a two-layer pigmentary unit comprising approximately 36 keratinocytes for every melanocyte[5]. Additionally, melanosomes form a ‘melanin cap’ to protect keratinocyte nuclei from harmful UV light[1].

1.1.2 The Dermis

The dermis is responsible for the various regional differences in skin thickness since it lies between the epidermis and subcutis[3]. The dermis consists of interstitial and cellular components, blood vessels, lymphatic channels and nerves and therefore plays a significant role in functions such as thermoregulation and immunity [1].

1.2 Skin cancer

Skin cancer is one of the most commonly occurring malignant neoplasms in light skinned populations[6]. Moreover, the incidence of melanoma and non-melanoma skin cancers is increasing worldwide[7, 8]. Malignant non-melanoma skin cancers including basal cell carcinoma (BCC) and squamous cell carcinoma (SCC) originate from keratinized epithelial cells, whereas melanoma skin cancers originate from melanocytes found at the basal layer of the epidermis[9]. Although these cancers have a relatively low incident rate in dark-skinned individuals, 5-year survival rate in this population remains poor[10].

The most common cause of developing melanoma or non-melanoma skin cancer is increased exposure to ultraviolet (UV) light[11]. Also, inherited genetic mutations including xeroderma pigmentosa are a cause[3]. In addition, the amount of melanin and an increasing number of atypical nevi (moles) pose significant risk for the development of melanoma[11].

1.3 Melanoma overview and epidemiology

Melanoma is an invasive and aggressive form of skin cancer known for its increased multidrug resistance, low rates of patient survival and tendency to relapse easily when diagnosed and treated late[12]. It is a neoplasm of the melanocytes found in the basal layer of the epidermis and develops as a result of accumulated abnormalities in genetic pathways of the melanocyte and eventually results in abnormal cell growth[13, 14]. In fact, genetic studies identified mutations/alterations in genes that activate the mitogen-activated protein kinase (MAPK) pathway with different changes across stages of tumour progression. The MAPK pathway involves a group of protein kinases that regulate cellular programs related to proliferation, differentiation and survival in response to changes in the cell environment[13].

Although melanoma accounts for approximately 4% of all dermatologic cancers , it is responsible for 80% of deaths related to skin cancers[15]. According to the World Cancer Research Fund, melanoma was ranked the 19th most commonly occurring cancer in men and women, with nearly 300,000 new cases worldwide in 2018[16]. In 2019 the five year prevalence for both male and females was predicted to be approximately 965 000 worldwide by 2024[17]. The morbidity and mortality rate of melanoma warrants

further investigation of mechanisms that contribute to the development and progression of the cancer.

1.4 Development and progression of melanoma

Histological studies of melanomas indicate that melanoma occurs de novo or could arise from pre-existing nevi[18]. The development and progression of melanoma can follow a stepwise process, preceded by adequate accumulation of genetic mutations in the melanocyte[13]. The Clark model describes six clinically and histologically evident lesional steps: (1) the development of benign nevi as a result of the acquired genetic alterations in the melanocyte, (2) dysplastic nevi, (3) radial growth phase (RGP) melanoma, (4) vertical growth phase (VGP) melanoma, (5) oinvasive melanoma, and (6) finally, metastatic melanoma[15]. Additional genetic mutations occur through the intermediate lesions leading to the RGP characterised by lesions within the epidermis which may sometimes present clinically as raised lesions[15, 19]. Furthermore, RGP may progress into the VGP where the direction of growth changes from a clinical plaque lesion to a nodule. This occurs because nests of melanoma cells grow beyond the basal membrane into the dermis (Figure 1.1)[13, 15, 19]. Since the dermis consists of blood vessels, the VGP is considered a threat for metastasis[20].

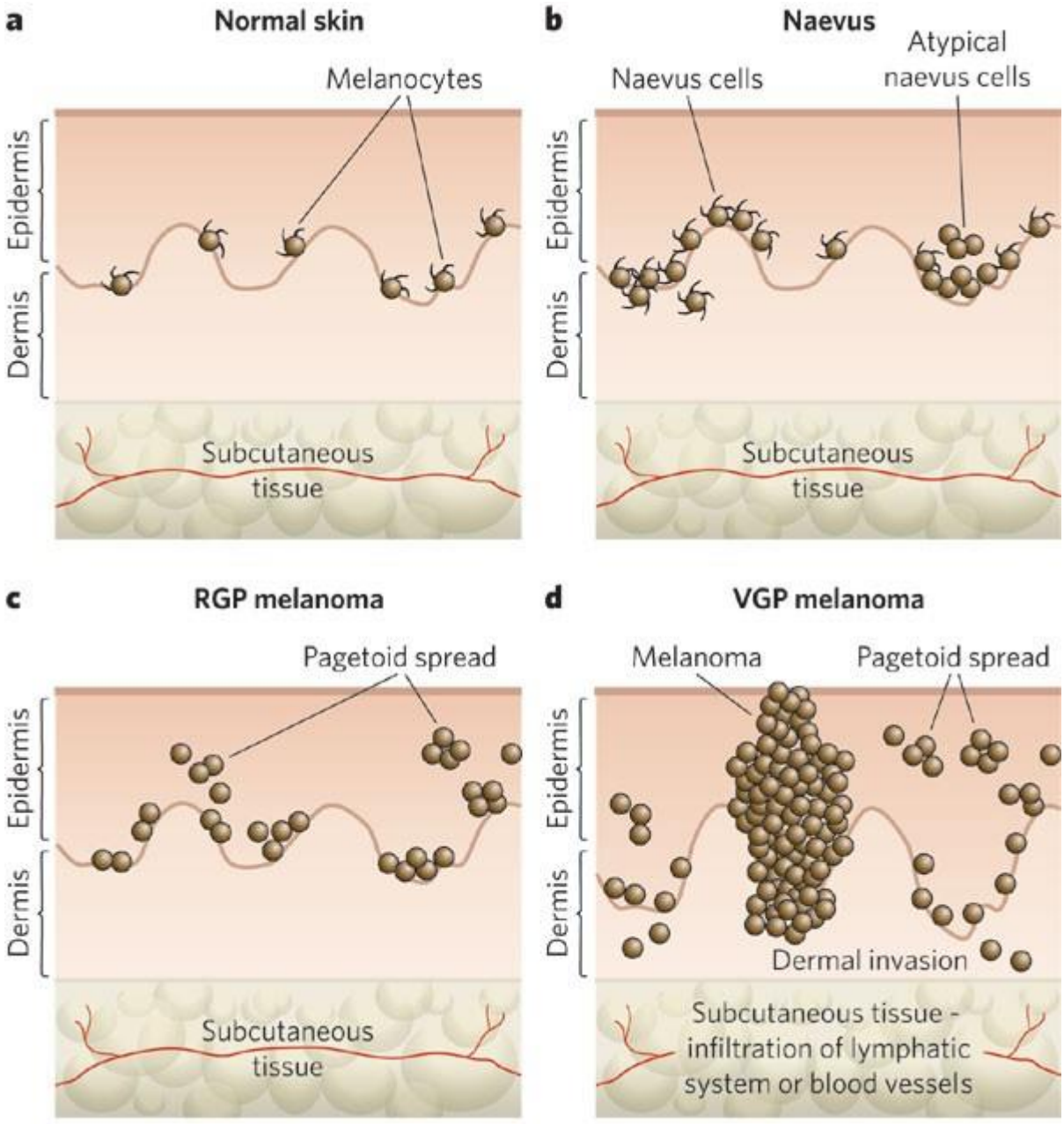

Figure 1.1 Progression of melanocyte transformation. There are various stages of melanocytic lesion, each of which is marked by a new clone of cells with growth advantages over the surrounding tissues. a) Normal skin - has an even distribution of dendritic melanocytes within the basal layer of the epidermis. b) Nevi - in the early stages, benign melanocytic nevi occur with increased numbers of dendritic melanocytes. According to their localisation, nevi are termed either junctional, dermal or compound. Some nevi are dysplastic, with morphologically atypical melanocytes. c) Radial-growth-phase (RGP) melanoma – RGP is considered to be the primary malignant stage. d) Vertical-growth-phase (VGP) melanoma - VPG is the first stage

that is considered to have malignant potential and leads directly to metastatic malignant melanoma, the deadliest stage, by infiltration of the vascular and lymphatic systems. The upward migration or vertical stacking of melanocytes is a histological characteristic of early metastatic melanoma. Adapted from Gray-Schopfer et al[19].

1.5 Diagnosis and staging of melanoma

The general consensus among guidelines for melanoma management is to consider melanoma diagnosis (Figure 1.2) in all pigmented or changing lesions on the skin. Suspicion of pigmented lesions is usually assessed using the 'ugly duckling' concept, which helps identify melanoma because nevi in the same individual tend to resemble one another, and melanomas often do not fit the individual's nevus pattern [21]. Another method of assessment uses the 'ABCDE' (Asymmetry, Border irregularities, Colour variation, Diameter, and Elevated surface) rule which functions to facilitate the diagnosis of early melanoma [21].

Furthermore, in order to enhance the accuracy of melanoma clinical diagnosis, it is recommended to use dermoscopy [22]. Dermoscopic diagnosis is based on assessment of specific criteria and the application of different diagnostic algorithms such as the ABCDE rule [21]. Other advanced systems like the automated melanoma diagnosis system termed MEDS, utilise machine learning-based classification algorithms to analyse lesion characteristics, including asymmetry, border irregularity, colour variation, diameter, and dermoscopic patterns to provide accurate diagnosis could be used [23].

Histologic features, such as Breslow's tumour thickness, ulceration or mitoses of primary melanoma in particular are considered independent important markers for melanoma prognosis [22, 24]. And, according to the ESMO clinical practice guidelines for diagnosis, treatment and follow up, melanoma diagnosis should be based on a full thickness excisional biopsy with minimal side margins. This is followed by histological confirmation and molecular characterisation whereby mutation testing of BRAF is mandatory [25]. Additionally, the rate and extent i.e. cancer stage is described [25].

There are 5 main stages of melanoma and the prognosis worsens with advancing stage (Figure 1.3)[26]. Clinico-pathologic staging of melanoma is based on the American

Joint Committee on Cancer (AJCC) criteria [27]. With this criterion, each of the letters T, N, and M describe a different area (i.e. primary tumour, regional lymph nodes and metastasis) of cancer growth based on clinical and pathological tests carried throughout melanoma diagnosis[20, 22]. Therefore, timeous and accurate diagnosis of melanoma is crucial for treatment planning and success [28].

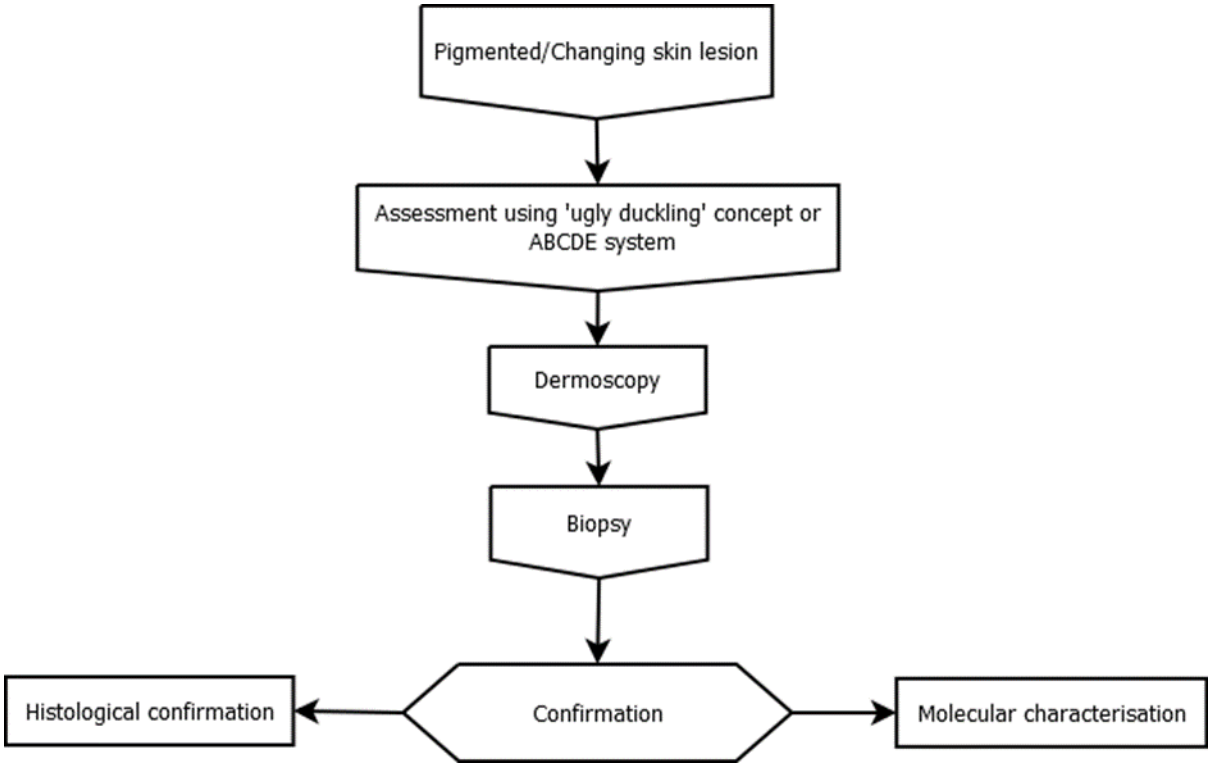

Figure 1.2 The process of melanoma diagnosis. The ABCDE system and dermoscopy are used to assess changing skin lesions, and diagnosis is confirmed by histopathological examination of a biopsy.

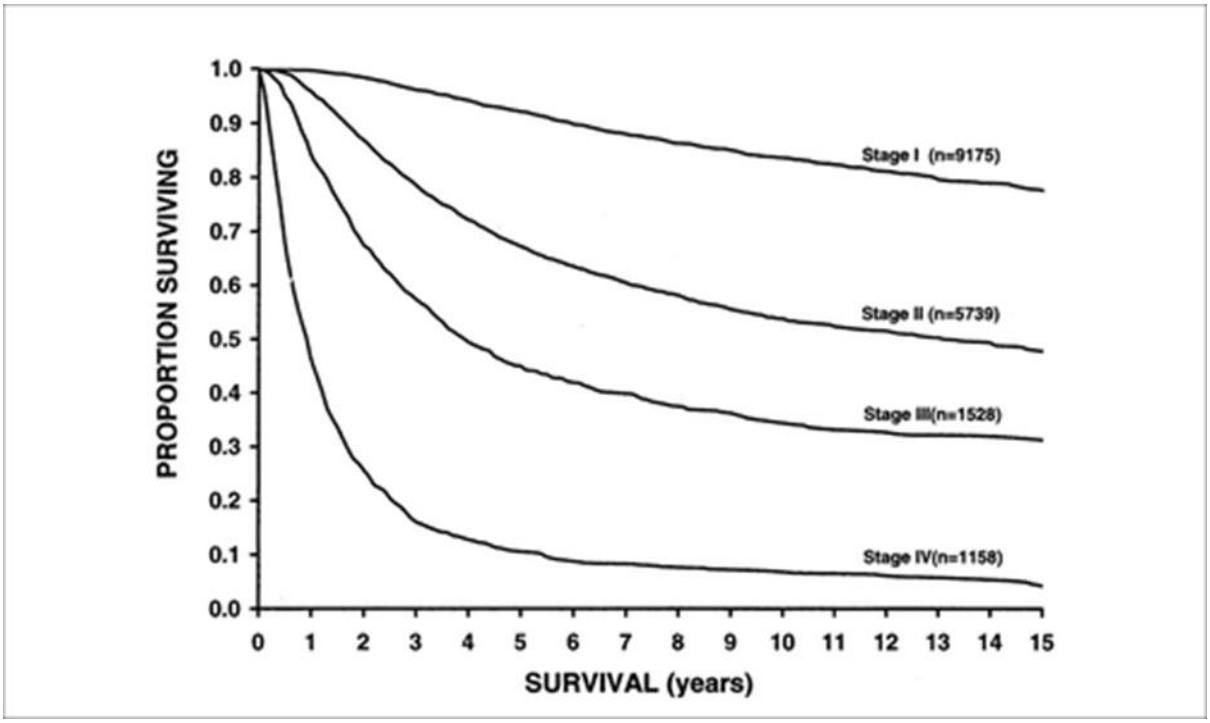

Figure 1.3 Fifteen-year survival curves comparing localised melanoma (stages I and II), regional metastases (stage III), and distant metastases (stage IV). The numbers in parentheses are the numbers of patients from the AJCC melanoma staging database used to calculate the survival rates. The differences between the curves are significant (P <.0001). Adapted from Charles M. Balch et al [26]

1.6 Management and treatment of melanoma

Various modalities are available for melanoma management depending on features of the tumour (*i.e.* location, stage and genetic profile), ranging from surgical resection, chemotherapy, radiotherapy, immunotherapy and targeted therapy[28]. Moreover, melanoma treatment options have progressively increased with advances in understanding the molecular pathogenesis. However, it is clear that single treatment is unlikely successful for some patients as a result of melanoma tumours being highly aggressive and hyper mutable [29, 30]. To overcome these features, a synergy between strategies including chemotherapy, immunotherapy and targeted therapy appears to be an appropriate approach by targeting different pathways [28].

1.6.1 Chemotherapy offers benefit to some extent

Chemotherapy is the earliest treatment option for advanced melanoma and remains important in palliative treatment of refractory, progressive and relapsed melanomas [28]. Dacarbazine in particular, continues to be used for the treatment of metastatic melanoma as approved by the U.S. Food and Drug Administration since it has demonstrated response rates between 15 to 25% with median response durations of 5 to 6 months when investigated in single-institution trials. Furthermore, long-term follow-up of patients treated with dacarbazine alone shows that <2% of patients can be anticipated to survive for 6 years[31].

Other agents such as cisplatin and carboplatin have shown modest activity as single agents for the treatment of metastatic melanoma with response rates of 15% and 19% with a partial median duration of approximately 4 and 7.58 months for cisplatin and carboplatin respectively[31]. Single-agent chemotherapy regimens have only shown modest activity in the treatment of metastatic melanoma. As a result, combination therapies have been evaluated in clinical trials. However, while at least one chemotherapy combination demonstrated some effect, the overall clinical effect was not sufficient to advocate this route due to high toxicities [31]. Conversely, alternative treatments including immunotherapy and targeted therapy have been evaluated [29].

1.6.2 Immunotherapy and Targeted therapy offer alternative treatment

The first FDA-approved immunotherapy indicated for metastatic/un-resectable cutaneous melanoma includes anti-PD-1 drugs (nivolumab, pembrolizumab), and anti-CTLA4 (Ipilimumab). Ipilimumab was the first agent to show significant survival rates in patients with metastatic malignant melanoma with response rates between 5 and 15% when used as monotherapy. Even greater effectiveness when immunotherapy agents, including ipilimumab, are used in combination with chemotherapy agents [32].

Approximately 50% of patients with melanoma have a mutation at the BRAF gene which is responsible for continued cell proliferation [33]. Besides the use of immune checkpoint therapy, targeted therapy which includes BRAF and MEK inhibitors is available. Vemurafenib, has shown promising results *in vivo* and *in vitro* with observed response rates of 69% in phase I clinical trials [29]. As seen in other types of cancer,

combination therapy remains pertinent and has been studied in advanced melanoma. This includes combining BRAF and MEK inhibitors in patients with a V600E mutation in the BRAF gene or combining immune checkpoint blockade therapy. Both approaches have resulted in significant increase in survival among patients compared with monotherapy[34].

Vascular endothelial growth factor-A (VEGF-A) plays an integral role in tumour angiogenesis and its inhibition results in suppressed tumour growth in murine models [35]. Bevacizumab is a monoclonal antibody targeting VEGF-A, and has been approved for use in breast cancer, non-small cell lung cancer, renal, ovarian, cervix and colorectal cancer [28, 36].

In single-arm phase II clinical trials, bevacizumab in combination with temozolomide was administered to patients with previously untreated metastatic melanomas resulting in a progression free survival of 4.2 months and an improvement in odds of survival (OS) in melanoma patients with a BRAF V600E mutation[37]. In another single-arm phase II study, bevacizumab in combination with IFN α2b was given to previously untreated melanoma patients. A progression free rate of 4.8 months was observed, indicating the potential of VEGF-A as a target, despite validation of this therapy for melanomas [28]. An ongoing clinical trial (NCT03175432) aims to determine the effect of bevacizumab in combination with chemotherapy agents in untreated melanoma that has spread to the brain. Though not the only trial, other clinical trials investigating the effect of bevacizumab in combination with immunotherapies are also being conducted [28].

Although various studies have demonstrated efficacy of anti-angiogenic agents in extending survival of cancer patients by few months, worryingly, the rate of recurrence and off-target toxicities remains high. Also, as with other cancer therapies, tumours can adopt various mechanisms of resistance including the upregulation of compensatory/alternative mechanisms of angiogenesis, vasculogenic mimicry, and vessel co-option in order to receive oxygen and nutrients when their survival is under threat [38]. This literature review will provide background on the concept of vasculogenic mimicry, signalling pathways involved, and clinical relevance, particularly in melanoma.

1.7 Vasculogenic mimicry promotes tumour growth and contributes to treatment refractoriness

Vasculogenic mimicry (VM) is a term used to describe the formation of tubular-like structures or highly patterned matrices in highly aggressive tumour cells[39, 40]. Unlike vasculogenesis or angiogenesis, where formation of vessels occurs *de novo* or from pre-existing vessels respectively and lined by endothelial cells[41], VM channels are lined with tumour cells as demonstrated by immunohistochemical staining of periodic acid Schiff (PAS) positive melanoma tissue sections[39]. This makes VM a novel paradigm of tumour perfusion and hence the term “vasculogenic” to describe the *de novo* formation of the channels by aggressive tumour cells and “mimicry” to emphasise the fact that the phenomenon is not a true vasculogenic event [41].

Although cutaneous melanoma is more prevalent, its progression and metastasis can occur through lymphatics and blood vessels[41]. The discovery of VM was initially observed in uveal melanoma, which lacks lymphatics but can still spread to other organs, such as the liver. This characteristic makes uveal melanoma an ideal model for studying the cellular and molecular architecture of melanoma microvasculature without the confounding influence of lymphatic circulation [39, 41].

Previous studies have identified the number of vessels and PAS-positive microcirculation patterns resulting from remodelling events as histological markers of tumour progression [39]. Furthermore, these patterns have been shown to be rich in laminin, collagen type IV, collagen type VI and glycosaminoglycans. The patterns consisted of arcs with and without branching, loops, networks, and straight linear deposits[40]. Similar patterns were observed in highly aggressive primary and metastatic uveal melanoma *in vitro*. Interestingly, such were without endothelial cells, fibroblasts, or soluble growth factors when compared with less aggressive melanoma cell lines, which did not form similar patterns [42].

1.7.1 Histological characteristics of vasculogenic mimicry

In vitro observations define two different types of VM including tubular and patterned matrix type [40]. Patterned VM is composed of an extracellular matrix of irregular thickness and stains positive for PAS, much like previously described types of tumour

microcirculation since they are rich in laminin or heparin sulfate. In addition, the islets of cancer cells are found surrounding the patterned matrix [39, 40]. In contrast, tubular VM is composed of tumour cells with phenotypic features of endothelial cells to form hollow structures and have the ability to conduct fluid [43]. Moreover, tubules formed by tumour cells were shown to be resting on an inner glycoprotein-rich matrix [39]. In tumour samples, VM is characterised by PAS-positive staining and negative immunohistochemistry analysis of either CD34 or CD31, two classical endothelial cell markers, since VM channels are lined by tumour cells and not endothelial cells [39, 44]. Furthermore, *in vitro* studies have confirmed the molecular characteristics underlying VM in which models of highly invasive melanoma cell lines were able to form VM in 3D culture [39]. Patterns formed by aggressive tumour cells also showed to be a component of tumour microcirculation as they were consistently traced back to blood vessels and laser scanning confocal angiography also demonstrated that these patterns conducted fluid movement [40, 45].

Results from the landmark study by Maniotis et al[39] also report on the cellular and molecular mechanisms underlying VM formation by highly aggressive melanoma cells and revealed that tumour cells that generate patterned vascular channels are deregulated and aberrantly express genes associated with embryonic stem cells including those associated with primordial vascular development [39]

1.8 Molecular regulators implicated in vasculogenic mimicry signalling

Potential molecular mechanisms involved in VM include epithelial-to-mesenchymal transition (EMT), cancer stem cells (CSCs) and the extracellular microenvironment [44]. Additionally, gene expression analysis studies demonstrate that highly aggressive melanoma cells exhibit features of endothelial cells when compared with poorly aggressive melanoma cells. Furthermore, genes involved in angiogenesis and vasculogenesis such as VE-cadherin, ephrin type-A receptor-2 (EphA2) and laminin 5γ2 chain were found to be upregulated in highly aggressive melanoma cells and thus the ability to engage in VM [46, 47]. Genes like Nodal and Notch4, as well as hypoxia-inducible factor (HIF) and Twist 1 as associated with embryonic and hypoxia-related signalling pathways respectively, are also implicated in VM formation (Figure 1.7) [38].

1.8.1 Interaction of VE-cadherin & ephrin type-A receptor 2 promote vasculogenic mimicry

Vascular endothelial cadherin is an important player of VM and was one of the first molecules identified in melanoma VM [48]. It is a calcium dependent protein and has a major role in cell-cell adhesion specifically for ECs [49]. Functional studies and morphological analyses performed in three-dimensional culture to test the hypothesis that upregulated VE-Cadherin expression by highly aggressive melanoma cells plays a role in vascular network formation. The results indicated that highly aggressive melanoma cells form a vascular pattern of cord-like networks much like networks formed *de novo* by angioblasts. In contrast, poorly aggressive melanoma cells expressing low levels of VE-Cadherin do not form such networks under similar culture conditions [47]. Also, VE-cadherin has been shown to promote VM formation in aggressive melanoma through interaction with ephrin type-A receptor 2 (EphA2), a receptor tyrosine kinase and member of the Eph family of protein tyrosine kinases by mediating its ability to become phosphorylated through interactions with its membrane bound ligand, Ephrin-A1 [50-52]. Phosphorylated EphA2 leads to the activation of Phosphoinositide 3-kinase (PI3k). Activated PI3k further induces the expression and activation of pro-membrane type 1 matrix metalloproteinase (MT1-MMP), which in turn activates matrix metalloproteinase 2 (MMP-2). MT1-MMP together with MMP-2 promote the cleavage of laminin 5γ2 chain into its promigratory γ2' and γ2x fragments which when released into the tumour microenvironment can increase migration, invasion and ultimately vasculogenic mimicry of aggressive melanoma tumour cells[53]. Another study showed that in melanoma cells, activation of focal adhesion kinase (FAK) increased the expression of VE-Cadherin and was positively correlated with VM formation[49]. Therefore, the interaction between VE-cadherin and EphA2 or inhibition of PI3k signal pathway serves as a potential target for anti-VM formation therapies in melanoma.

1.8.2 Vascular endothelial growth factor-A (VEGF-A) and Phosphoinositide 3 kinase (PI3k) are required for the formation of vasculogenic mimicry in melanoma

Members of the vascular endothelial growth factor family and their receptors are considered the main molecular drivers of angiogenesis. They include VEGF-A, VEGF-B, VEGF-C, VEGF-D and placental growth factors-1 and -2 [38]. Among these growth factors, VEGF-A is known to regulate vascularisation and is critical for EC division, migration and survival, especially when it interacts with its cognate receptor, vascular endothelial growth factor receptor 2 (VEGFR-2) [36].

Interestingly, VEGF-A has been implicated in the formation of vasculogenic mimicry in melanoma cells, whereby it stimulates the activation of PI3k by binding to vascular endothelial growth factor receptor 1 (VEGFR-1) depending on the activation of protein kinase C (PKC) [54]. As such, the integrin signalling pathway involving VEGF-A/VEGFR1/PI3k/PKC is essential for VM formation in melanoma cells [44, 54]. Furthermore, inhibition of VEGFR-1 using siRNA has been shown to disrupt VM formation [54]. Recently, a study investigating the effect of VEGF-A on VM formation in choroidal melanoma through the PI3k pathway demonstrated that blocking VEGF-A with siRNA reduced the activation of PI3k pathway and subsequently inhibited VM formation [55].

The role of VEGF-A signalling in mediating VM remains enigmatic. Given that, under normal physiological conditions, the expression of VEGF-A is associated with endothelial cell proliferation and tube formation when bound to VEGFR-2 and possibly angiogenesis [52]. Pertinent for melanoma VM, elucidating the expression of VEGF-A at different stages of melanoma in correlation with the presence of vasculogenic mimicry could unravel its clinical relevance as a marker of disease progression in melanomas treated initially with anti-VEGF therapies.

1.8.3 Nodal expression in melanoma cells is associated with features of vasculogenic mimicry

Nodal is an embryonic morphogen belonging to the transforming growth factor β (TGF-β) superfamily and is an example of a stem cell protein associated with cancer [56]. The

expression of Nodal is normally restricted to embryonic lineages and is responsible for embryo patterning. Additionally, nodal maintains the stemness of embryonic stem cells [56]. Interestingly, Nodal protein expression is absent in normal skin and rare in poorly invasive RGP melanomas. Conversely, Nodal protein has been detected in up to 60% of invasive VGP melanomas and melanoma metastasis cases by immunohistochemistry.[57] Also, Topczewska [57] have demonstrated that Nodal plays a fundamental role in maintaining the pluripotency and tumorigenicity of melanoma cells. Furthermore, western blot analysis of tumorigenic melanoma cell lines (C8161, WM793, and 1205 Lu) have shown high levels of Nodal, whereas, in normal melanocytes and non-tumorigenic melanoma cells (C81-61), Nodal expression was absent, illustrating a positive correlation with melanoma tumour progression [57, 58].

Of note, given the evidence that Nodal plays a significant role in clinical progression of melanoma, studies have associated Nodal expression with features of VM *in vitro* and *in vivo.* One example is that of a humanised murine xenograft model in which developing human melanomas may be studied sequentially during the early stages of tumorigenic growth within a physiological human dermal microenvironment[59]. Through this model, McAllister [58] demonstrated that Nodal is expressed in melanoma nodules at an mRNA level in association with anastomosing channels with features consistent with VM. This association has also been suggested in a zebrafish model, where Nodal protein was shown to be expressed by injected human melanoma cells and had biological effects on both embryonic morphogenesis and the molecular pathway implicated in VM response [58]

Furthermore, treatment of aggressive melanoma cells with a function-blocking anti-Nodal antibody reduced their ability to engage in VM, suggesting the important role of Nodal as a regulator of tumour plasticity and the trans-endothelial phenotype [60]. Another study in support of the potential role of Nodal in VM formation also showed that inhibition of Nodal expression was associated with a decreased expression of VE-cadherin and subsequently hindered VM formation by melanoma cells[47]. Based on these studies, Nodal appears to play a crucial role in VM formation. Thus, further investigation of nodal expression at different stages of melanoma in correlation with the presence of VM may have clinical relevance and could potentially be used as a prognostic marker in VM-targeted therapies.

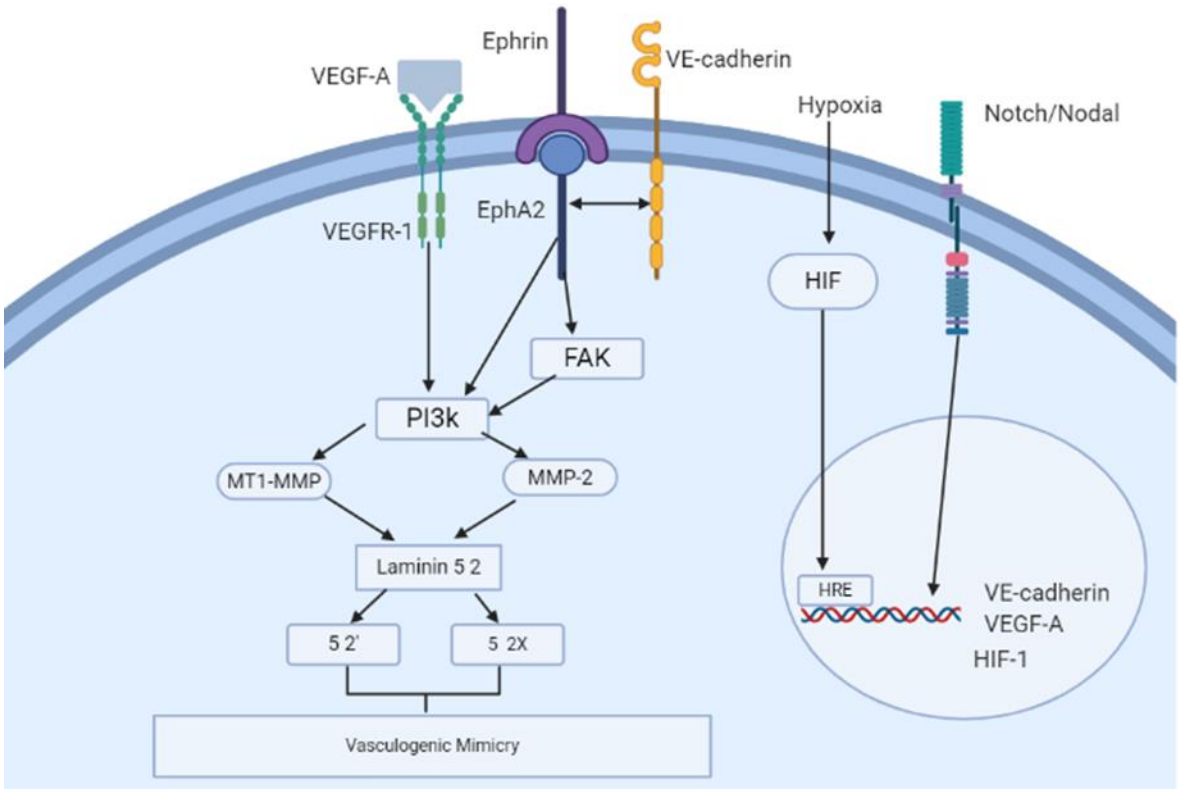

Figure 1.4 Vasculogenic mimicry signalling. VE-cadherin interacts with EphA2 to activate phosphoinositide 3 kinase pathway which leads to the activation of MT1-MMP and MMP-2 which in turn leads to the cleavage of Laminin 5γ2 into its promigratory factors and promigratory factors and promotes vasculogenic mimicry.

1.9 The presence of vasculogenic mimicry in melanoma is significantly associated with unfavourable clinical outcomes

Previously, the prognostic value of tumour blood vessel morphology in primary uveal melanoma showed a strong association between the presence of vascular channel-associated patterns in patient tissues and death from metastatic melanoma [39]. Since the discovery of VM by Maniotis et al [42] , various studies have been conducted in cancer patients, including melanoma, to investigate the clinical significance of VM on the progression of disease and overall survival.

The presence of PAS-positive patterns, a characteristic of VM, has been significantly associated with a decrease in disease-free outcomes in melanoma (Figure 1.8) [42]. In addition to existing evidence on the role of VM on metastasis in uveal malignant melanoma, Thies et al [61] analysed the relationship between the presence of VM and

metastasis in malignant cutaneous melanoma and showed that the presence of VM was strongly associated with metastasis and subsequently poor outcomes in contrast to the lack of VM in tumours[61]. Notably, a retrospective cohort study involving 123 melanoma patient tumour tissue samples further showed that the presence of VM was significantly correlated to metastasis[62]. In addition, immunohistochemical analysis of tissue samples from 118 melanoma patients showed that VM was present in a majority of melanomas and only a few cases of benign nevi, suggesting VM as a prognostic marker for melanoma progression [63]. Furthermore, an updated meta-analysis showed that VM is significantly associated with poor overall survival in cancer patients, including melanoma (Table 1.2). Moreover, the presence of VM is also significantly associated with clinical disease features such as lymph node metastasis, distant metastasis and TNM stage (Table 1.3) [64]. Also, VM has consistently been associated with poor prognosis in many types of cancer [65]. Furthermore, VM in colorectal cancer is considered a strong independent prognostic marker for survival [66]. Therefore, results from the aforementioned studies show that the presence of VM in tumour tissue samples of cancer patients, including melanoma, is of prognostic relevance and warrants further investigation to better understand molecular mechanisms involved in its formation and how they correlate with disease progression [39, 63, 64].

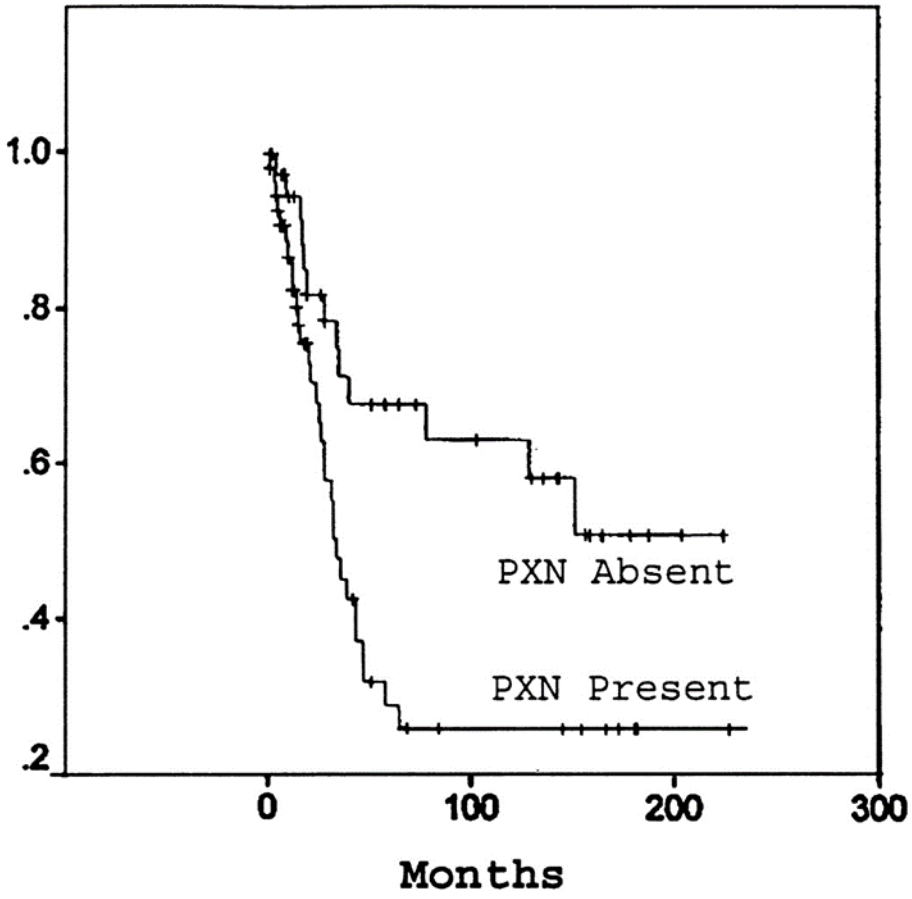

Figure 1.5 Kaplan-Meier survival curve for disease free survival of patients with primary cutaneous melanoma: comparison of patients whose tumours contained versus lacked parallel with cross-linking or network PAS-positive patterns (PXN). Adapted from Warso et al [64].

Tumour growth and metastasis are supported by sufficient blood supply; however, many antiangiogenic drugs targeting VEGF-A and subsequently blocking vessel growth have shown benefit in some patients and not others notwithstanding their limited use due to various side effects[67, 68]. VM is considered a potential mechanism contributing to anti-angiogenic therapy, possibly due to its ability to induce hypoxia. Hypoxia has been linked to VM formation, which in turn promotes continued tumour progression [38, 44]. In addition, previous studies have linked VM formation with less-differentiated subpopulations of cancer cells capable of phenotypic and functional plasticity and is further supported by the ability of melanoma subpopulations which have acquired chemoresistance to form VM [39, 69]. Furthermore, VM-rich regions of Merkel cell carcinoma, a rare and highly aggressive cutaneous neoplasm with a high

rate of morbidity and mortality have demonstrated resistance to conventional chemotherapeutic agents [70]. Therefore, VM formation is of clinical relevance and is a potential target for cancer therapy.

Table 1.1 Subgroup differences in a meta-analysis of the association between vasculogenic mimicry and disease features in patients with cancer. Adapted from Yang et al [64].

		Patients (n)					
Group	Studies (n)	VM+	VM-	RR (99 % CI)	P	I^2 (%)	P^a_{het}
Sex (female vs male)	17	592	1560	0.91 (0.74-1.12)	0.38	11.4	0.32
Differentiation (moderate/poor vs. well)	14	791	1241	1.08 (1.04-1.12)	<0.001	85.5	<0.001
Lymph metastasis (N1 vs N0)	10	458	1277	1.81 (1.43-2.29)	<0.001	75.4	<0.001
Distant metastasis (M1 vs. M0)	13	356	1260	1.94 (1.56-2.41)	<0.001	44.2	0.04
TNM stage (III/VI vs. I/II)	13	557	1358	1.81 (1.48-2.23)	<0.001	79.0	<0.001

1. *VM+* patients with positive vasculogenic mimicry, *VM-* patients without vasculogenic mimicry, *RR* risk ratio, P_{het} *P* values for heterogeneity from *Q* test

2. [a]A random-effect model was used when the *P* value for heterogeneity test was <0.05; otherwise, a fixed-effect model was used. I^2 the percentage of variability in RR attributable to heterogeneity

Table 1.2 Estimated effect of vasculogenic mimicry on overall survival in a meta-analysis of 36 studies of cancer patients by subgroup. Adapted from Yang et al [64]

Subgroup	Studies (n)	Patients		Overall survival, HR (95 % CI)	P [a]	I^2 (%)	P_{het}
		VM+	VM-				
Total	36	964	2645	2.16 (1.95 -2.38)	<0.001	29.4	0.055
Cancer type							
Melanoma	5	234	495	2.14(1.47-2.82)	<0.001	12.6	0.33
Gastric cancer	5	169	469	1.79 (1.23-2.94)	<0.001	31.3	0.21
Sarcomas	4	59	173	2.08 (1.23-2.94)	<0.001	0.0	0.59
Ovarian tumour	3	105	119	1.91 (0.63-3.18)	0.003	0.0	0.49
HCC	2	36	151	2.18 (1.36-3.00)	<0.001	0.0	0.55
Breast cancer	2	52	369	2.40 (0.85-3.95)	0.002	77.1	0.04
HNC	2	85	230	3.06 (1.85-4.27)	<0.001	0.0	0.73
Colorectal cancer	2	62	258	2.57 (1.72-3.42)	<0.001	61.8	0.11
Glioma	2	126	230	2.05(1.26-2.85)	<0.001	0.0	0.36
Lung cancer	2	126	230	2.05 (1.26-2.85)	<0.001	0.0	0.46
Other[a]	6	187	384	3.05 (2.45-3.64)	<0.001	44.6	0.11
Ethnicity							
Asian	31	965	2746	2.13 (1.91-2.35)	<0.001	28.8	0.07
Non-Asian	4	193	339	3.45 (2.13-4.77)	<0.001	0.0	0.52
Assay methods							
PAS	7	285	801	2.25 (1.68-2.82)	<0.001	13.7	0.33

CD31/PAS	14	341	1044	2.11 (1.67-2.54)	<0.001	25.0	0.18
CD34/PAS	13	491	1169	2.15 (1.87-2.43)	<0.001	48.1	0.03
Pan-cytokeratin/CD34	1	41	71	2.84 (1.09-4.59)	0.002	NA	NA
Sample size (n)							
≤100	16	756	2170	2.01 (1.74-2.29)	<0.001	1.6	0.43
>100	19	402	915	2.43 (2.07-2.78)	<0.001	39.3	0.04
Study quality [c]							
Low quality	17	506	1535	2.47 (2.13-2.81)	<0.001	42.2	0.03
High quality	18	652	1550	1.97 (1.67-2.23)	<0.001	0.0	0.60

1. *VM+* patients with positive vasculogenic mimicry, *VM-* patients without vasculogenic mimicry, *HR* hazard ratio, I^2 the percentage of variability in attributable to heterogeneity, P_{het} *P* values for heterogeneity from *Q* test, *HCC* hepatocellular carcinoma, *HNC* head and neck cancer, *PAS* Periodic acid-Schiff staining, *NA* not available
2. [a]A random-effect model was used when the *P* value for heterogeneity was <0.05; otherwise, a fixed-effect model was used
3. [b]Other included testicular germ cell malignant tumours, gallbladder cancer, prostate cancer, oesophageal cancer, renal carcinoma, and osteosarcoma
4. [c]Low-quality studies had Newcastle-Ottawa quality scores of 0-4, and high-quality studies had scores of 5-9

1.10 Therapeutic approaches targeting vasculogenic mimicry in melanoma

Efforts to inhibit VM formation have explored various mechanisms, including the use of antibodies targeting MMP-2 or MT1-MMP, the downregulation of VE-cadherin, and the inhibition of other VM-associated regulators [68]. Additionally, several agents targeting molecular regulators of VM have demonstrated efficacy in both *in vivo* and *in vitro* studies [65]. Notably, inhibitors of key VM regulators such as Nodal and EphA2 have shown promise in other cancers, where their inhibition was associated with a reduction in VM formation[52].

However, the effectiveness of antiangiogenic drugs targeting VEGF-A, such as endostatin, has been limited in suppressing VM formation in melanoma cells [71]. Despite these limitations, other agents like Rapamycin and CVM-1118, which target VEGF-A and other molecules, are under clinical development [52]. In melanoma specifically, compounds such as Thalidomide and Genistein, which target MMPs and VE-cadherin respectively, have been found to inhibit VM formation, highlighting the potential of these molecular targets in addressing VM [72].

1.11 Study rationale

Melanoma is a highly aggressive form of skin cancer with a high potential for metastasis and resistance to conventional therapies. One of the key mechanisms that contribute to melanoma progression is VM. Currently, there are drugs undergoing clinical development with the potential to inhibit VM and metastasis in melanoma. However, further investigation into the molecular mechanisms underlying VM is essential to support the development of alternative therapeutic strategies aimed at improving patient outcomes.

1.12 Aims and Objectives

1.12.1 Aim

The aim of this study was to examine the presence of vasculogenic mimicry markers in melanoma tissue and to evaluate the effects of VEGFR-1 blockade on various parameters of melanoma vasculogenic mimicry *in vitro*.

1.12.2 Objectives

The objectives of this study are:

- To determine the expression of VCAM-1 and VEGF-A in human melanoma using immunohistochemistry.
- To evaluate melanoma cell viability using the crystal violet assay.
- To study the morphology of aggressive melanoma cells using polarisation-optical interference (PlasDIC) microscopy.
- To evaluate melanoma cell migration and invasion using the scratch assay and the xCELLigence system.
- To determine the expression of the receptor that promotes VM, VEGFR-1 using western blot.

CHAPTER 2: MATERIALS AND METHODS

2.1 Study design

The study investigated the presence of VM in melanoma tissue obtained from eleven patients. Paraffin fixed melanoma biopsies derived from patients confirmed with melanoma diagnosis were obtained from the Department of Anatomical Pathology and utilised to evaluate the expression of VEGF-A and VCAM-1 in the melanoma biopsies using immunohistochemistry(Figure 2.1).

To complement the results from patient studies, *in vitro* studies were conducted using the B16-F10 melanoma cell line,a highly metastatic model known to exhibit VM[73]. The effect of VEGFR-1 blockade, a receptor implicated in promoting VM, was evaluated using sunitinib malate, a multi-kinase inhibitor with activity against VEGFR-1. Experiments included assessing cell viability using the crystal violet assay. Morphological changes were examined using polarisation-optical interference contrast microscopy (PlasDIC). Migration and invasion were studied through the wound scratch assay and the xCELLigence real-time monitoring system (Figure 2.1).

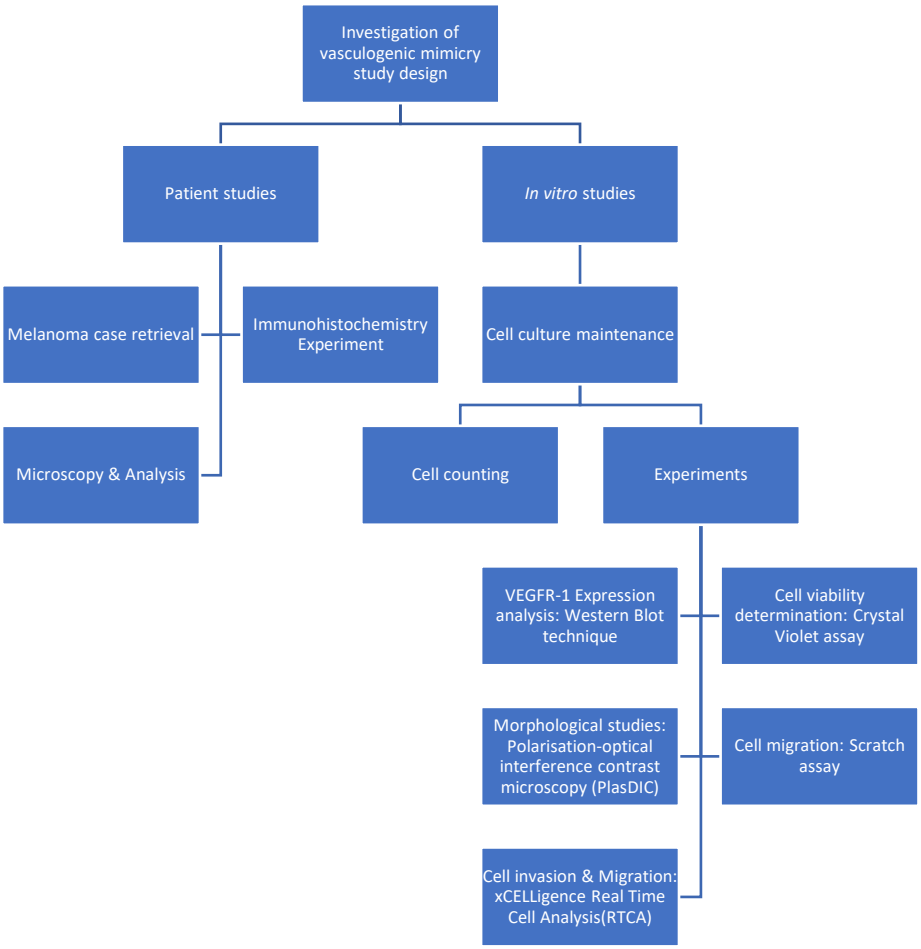

Figure 2.1 Flow diagram illustrating the study design.

2.2 Immunohistochemistry

Immunohistochemistry is a technique used in the diagnosis and research of infectious and neoplastic diseases. In principle, the technique enables the demonstration of tissue-specific antigens by staining with specific antibodies. The antibodies are labelled with either a fluorescent or enzymatic tag, which can be visualised under a microscope to locate target antigens (Figure 2.2) [74].

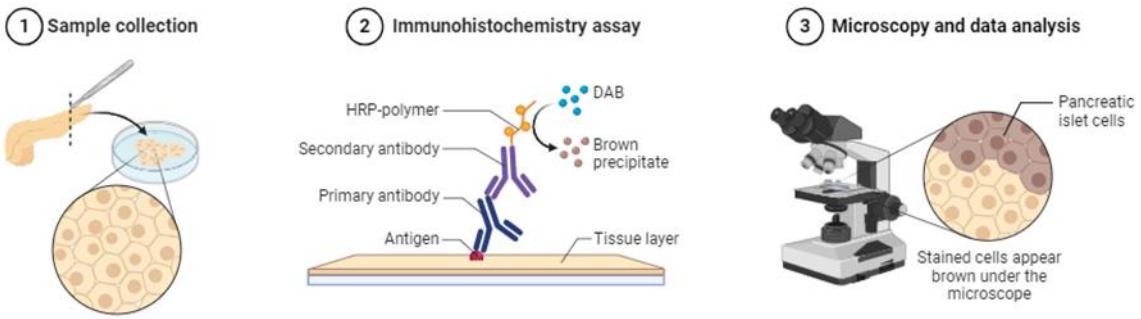

Figure 2.2 Summary of the immunohistochemistry (IHC) principle where (1) indicates sampled collection and preparation followed by (2) the IHC assay preceded by deparaffinization for paraffin sections and antigen retrieval. Where 3 illustrates microscopy and data analysis step.

Melanoma-derived paraffin sections of 4 µm were collected on Superfrost™ Plus Adhesion microscope slides (New Erie Scientific LLC, Portsmouth, NH, USA) and were baked for 1 hour (h) at 60 °C in an oven before deparaffinization. Thereafter, deparaffinization, antigen retrieval, blocking and detection were carried out in the Ventana Benchmark XT platform (Roche Diagnostics, Indianapolis, USA) using reagents purchased from Roche, Ventana Medical Systems, Tucson, AZ, USA. Human placenta tissue was used for antibody expression validation and subsequently used as a control for all study samples.

Paraffin sections were deparaffinised in EZ prep solution at 75 °C for 8 minutes (min). Thereafter, Heat Induced Epitope Retrieval (HIER) method for antigen retrieval was achieved using Conditioner #1, standard CC1 (Tris-EDTA buffer, pH 9) at 95 °C for 30 min. Endogenous peroxides and protein were blocked with Inhibitor CM for 4 min at 37°C. Tissue slides were then incubated with either rabbit polyclonal anti-VCAM1 (HPA034796, 1:100, Atlas Antibodies AB, Stockholm, Sweden) or rabbit polyclonal anti-VEGFA (HPA069116, 1:100, Atlas Antibodies AB, Stockholm, Sweden) primary antibody for 32 min. Thereafter, a chromogenic procedure was done using ultraView universal Alkaline Phosphatase Red Detection Kit (Ventana Medical Systems, Cat. No. 760-501) for 37 min. Counterstaining for nuclei was done by incubation with Haematoxylin II for 16 min, followed by Blueing reagent for post counterstain and incubated for 4 min. Thereafter, the slides were removed from the instrument and cleaned in warm water with a detergent. The slides were air-dried at room temperature

(RT) for 30 min and then covered with a coverslip in permanent mounting media. Images of intratumoral hotspots depicting expression and staining intensity of VEGF-A and VCAM-1 were captured using the Olympus DP74 digital camera mounted on an Olympus BX53 microscope (Olympus, Wendenstrasse, Hamburg, Germany) at 2x and 10x magnification respectively.

2.2.1 Immunoreactivity scoring

An experienced pathologist reviewed the sections following immunohistochemical staining to assess and score the expression of VEGF-A and VCAM-1. For this, intratumoral hotspots were found in low power fields and then measured the total scores of four intratumoral hotspots with high-power fields. A modified Allred Quick score, which is a combination of two parameters including, proportion and intensity scores was used (Table 2.1) where a score of 0-1 was considered negative, 2-3 as low, 4-5 as moderate and 6 to 8 as strong expression.

Table 2.1 Table illustrating the components of the Allred Quick score.

Allred Quick score Components			
Intensity	**Value**	**Proportion of cells positive**	**Value**
Negative (no staining of any nuclei at magnification)	0	0%	0
Weak (only visible at high magnification)	1	<1%	1
Moderate (readily visible at low magnification)	2	1-10%	2
Strong (strikingly positive at low magnification)	3	11-33%	3

	34-66%	4
	67-100%	5

2.3 Cell Culture Maintenance

The B16-F10 melanoma cell line was purchased from the American Tissue Culture Collection (ATCC, Manassas, Virginia, USA). The cells were grown in Dulbecco's Modified Eagle's Medium (DMEM) (Sigma-Aldrich, St Louis, MO, United States of America), supplemented with 10% foetal bovine serum (FBS) (Scientific Group, Midrand, South Africa), 2 mM L-glutamine (Whitehead Scientific, Johannesburg, South Africa) and 1% penicillin-streptomycin (Whitehead Scientific, Johannesburg, South Africa). The cell lines were maintained as monolayer cultures in sterile flasks (area 25 cm^2) at 37 ºC in a humidified atmosphere containing 5% carbon dioxide (CO_2) (Figure 2.3).

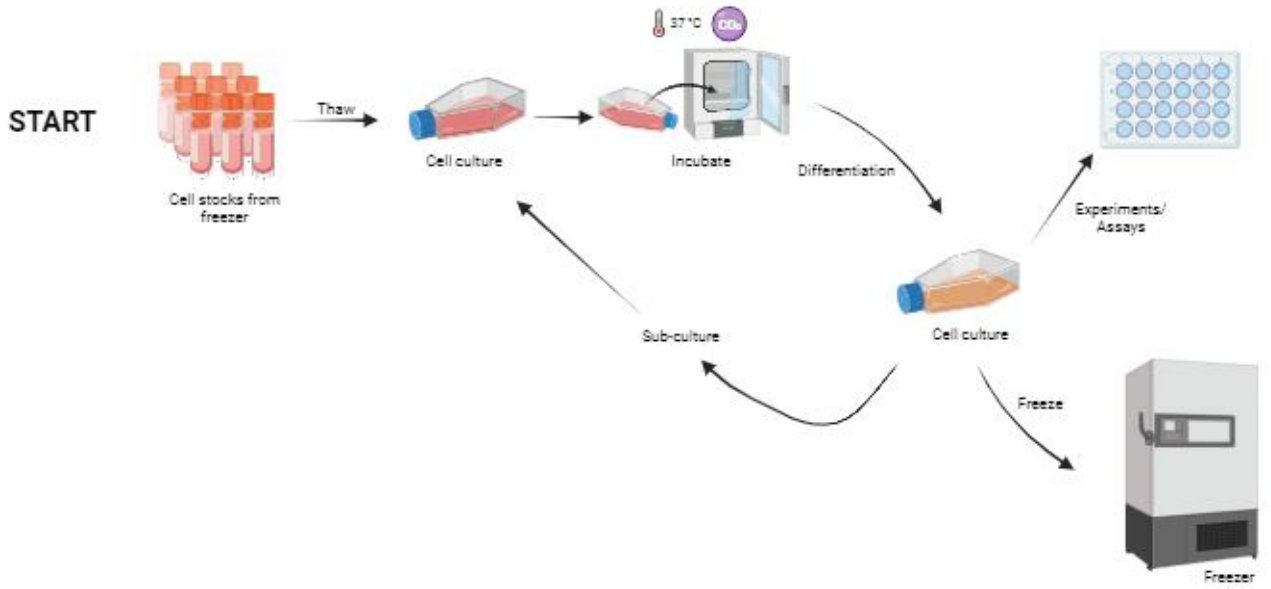

Figure 2.3 Basic illustration of cell culture maintenance under sterile conditions.

2.4 Cell Counting

Before experiments using cultured cells were conducted, viable cells from monolayer cultures were counted using a dye exclusion test. Principally, live cells with intact

membranes have the ability to exclude certain dyes such as trypan blue, eosin, or propidium, while dead cells lack this ability [75]. Therefore, trypan blue exclusion test was utilised in this study.

Cells from monolayer cultures were initially washed with pre-warmed 1X Phosphate buffered saline (PBS) solution and then treated with pre-warmed trypsin to enable detachment from the flasks. Following detachment, the mixture was transferred to a 15 mL centrifuge tube (Thermo Scientific, Johannesburg, South Africa) and centrifuged for 10 min at 2000 rpm at RT. After centrifugation, the supernatant was discarded, and the pellet was resuspended in DMEM. For cell counting purposes, the cell suspension was stained 1:1 with 0.2% trypan blue in PBS, loaded onto a haemocytometer (Figure 2.4) and visualised at 10 x magnification using the Zeiss Axiovert CLT 40 light microscope (Zeiss, Oberkochen, Germany) and thus counted unstained, viable cells and determined the cell density using the below formula and subsequently utilised the calculated cell density to seed for cell viability and proliferation assays.

$$Cell\ density\left({}^{cells}/_{mL}\right) = \frac{Total\ number\ of\ viable\ cells}{number\ of\ squares\ (4)} \times Dilution\ factor\ \times 10^4$$

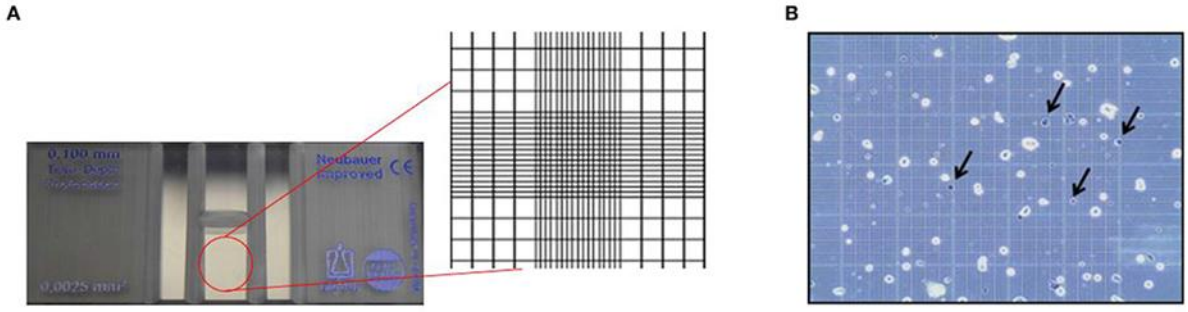

Figure 2.4 Illustration of the procedure for cell counting. (A) Zoomed inset of a haemocytometer showing the Neubauer chamber with a counting grid. (B) Illustration of the principle of trypan blue dye exclusion assay, where the arrows indicate dead cells [76]

2.5 Compound preparation

A stock solution of sunitinib malate (Sigma-Aldrich, St. Louis, MO, United States of America) at a concentration of 1 mg/mL was prepared in physiological saline. The stock solution was divided into microtubes and stored at -20 °C until needed. On the day of the experiments, drug dilutions were freshly prepared using cell culture medium.

2.6 Cell Viability Determination

Crystal violet is a dye which binds to proteins and deoxyribonucleic acid (DNA) and is utilised to study the behaviour of adherent cells, particularly cell survival and growth inhibition under various conditions such as time, exposure to chemotherapeutics and other compounds [77].

In this study, crystal violet assay was utilised to assess the growth of B16-F10 cells over 24- and 48-h using the previously described protocol with some modification [77].

The aggressive melanoma (B16-F10) cells were seeded in 96-well plates (Lasec, Cape Town, South Africa) at a density of 5 000 cells per well and were incubated at 37 ºC in a humidified atmosphere containing 5% CO_2 for 24 h to allow for attachment, and thereafter for 24- and 48-h following exposure to 0.1, 1, and 10 µg/mL of sunitinib malate or . Positive control cells were treated with physiological saline. Thereafter, the medium was removed and discarded. Adherent cells were fixed with 1% solution of glutaraldehyde (in H_2O) (Sigma-Aldrich, St. Louis, MO, United States of America) by incubation at room temperature for 15 minmin. Cells were then stained with 1% solution of crystal violet (in H_2O) for 30 min at RT. After 30 min, the plate was washed under running tap water and allowed to dry overnight. Thereafter, fixed and stained cells were solubilised with 100 µL of 0.2% Triton X-100 (Sigma-Aldrich, St. Louis, MO, United States of America) per well. The absorbance of samples was read at 570 nm on an ELx 800 Universal Microplate (BioTek instruments Inc, Weltevreden, South Africa)

2.7 Morphological studies

2.7.1 Polarisation-optical differential interference contrast

Polarisation-optical transmitted light differential interference contrast (PlasDIC) is a three-dimensional contrast approach for studying and viewing cell morphology. PlasDIC is an improved method where linearly polarised light is only generated after the objective and results in high-quality images of individual cells, cell clusters, and thick individual cells in plastic cell-culture tubes [78]. PlasDIC was employed to view and study the morphology of B16-F10 cells when treated with sunitinib malate and under physiological saline conditions for 24 h.

Exponentially growing B16-F10 cells were seeded in 6-well plates (Sigma-Aldrich, St. Louis, MO, United States of America) at a density of 300 000 cells per well and cultured overnight in a humidified incubator at 37 ºC supplemented with 5% CO_2 to enable cell attachment. Once cells have attached, the previous medium was removed and discarded and then cells were treated with sunitinib malate or medium and incubated for 24 h. Thereafter, PlasDIC images were captured at 40 x magnification using a Zeiss Axiovert MRm digital camera mounted on a Zeiss Axiovert 40 CFL microscope (Zeiss, Oberkochen, Germany).

2.8 Cell migration

2.8.1 *In vitro* scratch assay

The scratch assay is a standard, economical *in vitro* technique utilised to study cell migration in 2 dimensions. Principally, the technique involves the creation of a scratch/ “wound” on a confluent cell monolayer and subsequently capturing images of the “wound” width area at the beginning and at regular time intervals during cell migration to close the scratch (Figure 2.5) [79, 80]. Since vascular endothelial growth factor receptor-1 (VEGFR-1) is known to signal vasculogenic mimicry, the *in vitro* scratch migration assay was used to study the effect of VEGFR-1 blockade on the migration of B16-F10 cells.

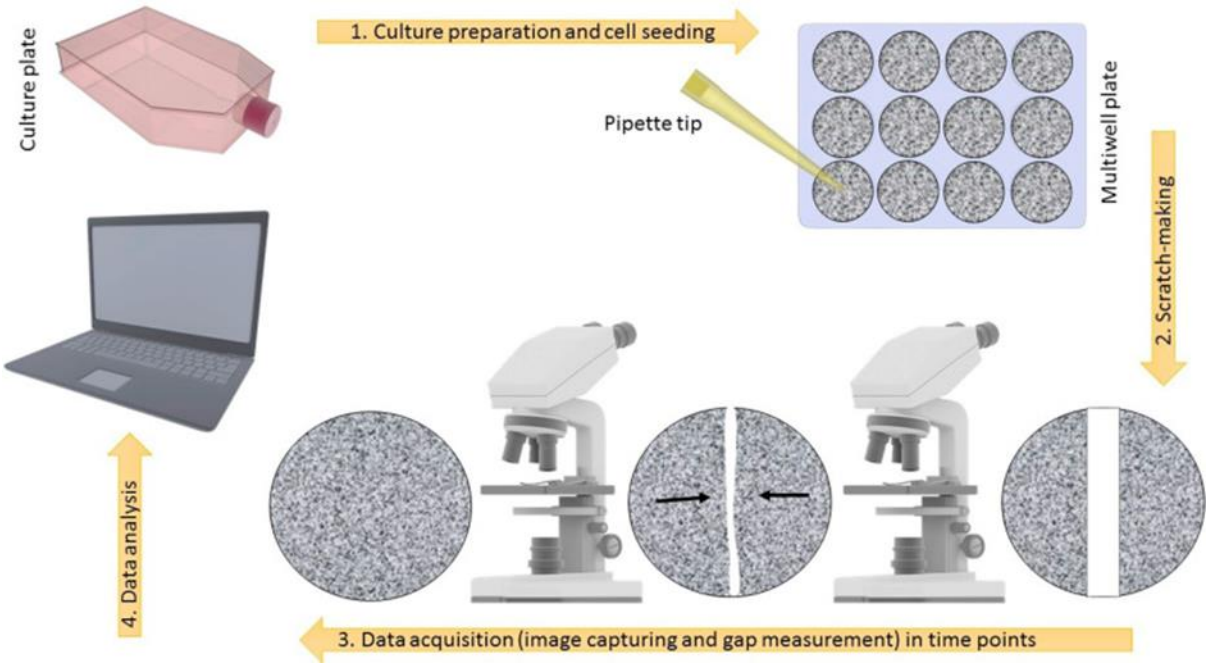

Figure 2.5 Graphical abstract summarizing the workflow of the *in vitro* would healing assay [81]

Exponentially growing B16-F10 cells from stock flasks were seeded in 6 well plates (Sigma-Aldrich, St. Louis, MO, United States of America) at a density of 300 000 cells per well and cultured overnight in a humidified incubator containing 5% CO_2 at 37 °C to enable cell attachment. At 100% confluence, the cell monolayer was scratched vertically and horizontally using a 10 µL yellow pipette tip. Thereafter, the cells were gently washed twice with 1X PBS to remove detached cells while performing scratch. Thereafter, the cells were treated with sunitinib malate (2.6 µg/mL and 5.2 µg/mL) or complete medium (DMEM) and incubated for 22 h in a humidified atmosphere containing 5% CO_2 at 37 °C. The scratch area was viewed using a Zeiss Axiovert CFL 40 microscope and images were captured at 5 x magnification at 0, 6, 12 and 22 h using a Zeiss Axiovert MRm digital camera (Zeiss, Oberkochen, Germany).

2.9 Cell invasion and migration (CIM)

The xCELLigence ® Real-Time Cell Analysis (RTCA) system was employed to measure cell proliferation. The system utilises electronic culture plates (CIM plates) with an upper chamber and a lower chamber equipped with gold microelectrodes at the bottom. This system measures impedance variations within an electrical circuit and translates them into a cell index (CI). The CI reflects the cell number, cell size, and the degree of cell attachment [82, 83]. Consequently, xCELLigence monitors the real-time dynamics of cells (Figure 2.6) [84]. In this study, the xCELLigence system was utilised to study melanoma cell invasion and migration into the lower chamber over a 22-hour (h) period. The cells double over 24-26 h, therefore the experiment was limited to 22 h.

Fifty microliters (50 µl) of medium were added to each well of the 16-well CIM plate (Agilent Technologies, Santa Clara, CA, USA) and incubated at RT for 30 min. Plates were placed into the xCELLigence® RTCA dual plate (DP) instrument (Roche Applied Science, Penzberg, Germany) for 30 min. A background impedance reading was taken. Then cells were seeded at density of 6000 cells/100 µl into the wells of the upper chamber of each 16-well CIM plate and incubated at RT for 30 min. Plates were then loaded onto the xCELLigence® RTCA DP instrument to measure the CI over 22 h.

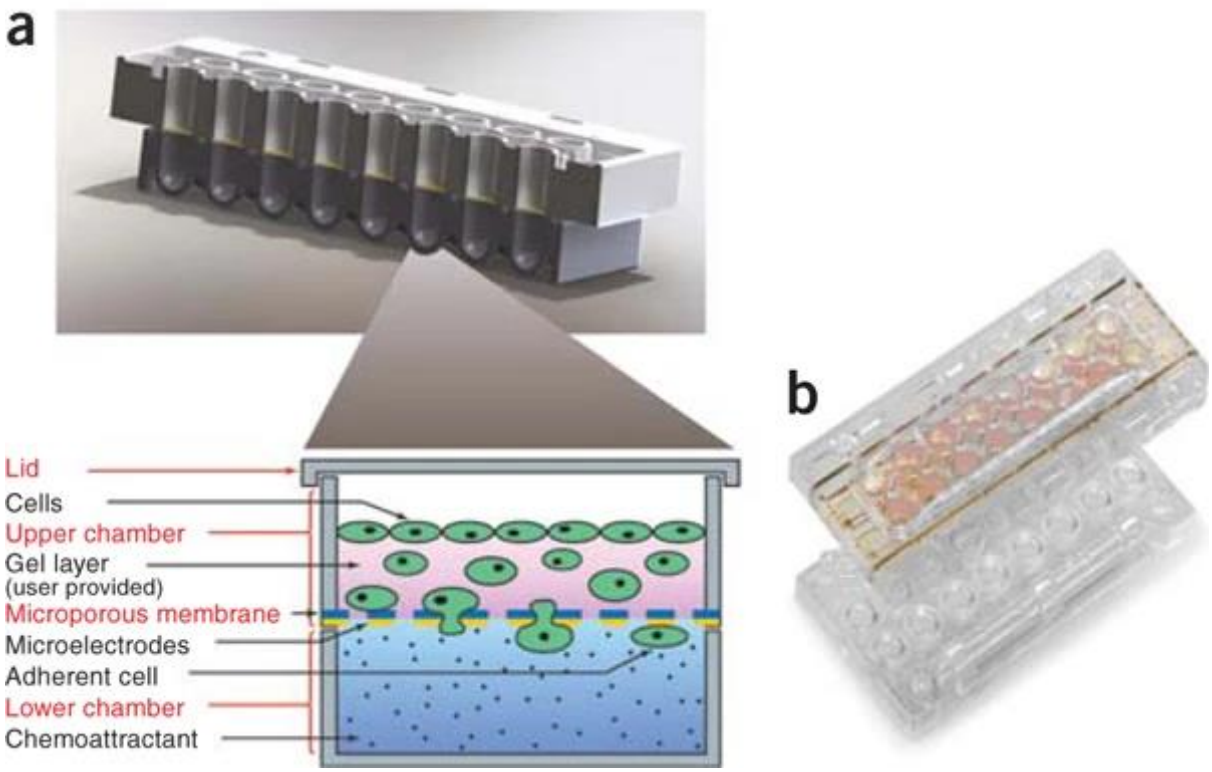

Figure 2.6 The CIM-plate 16 device for real-time cell invasion/migration analysis. (a) Graphical representation. The plate features two separable sections for ease of experimental setup. (b) The actual device is clear plastic [85]

2.10 Western blotting

Western blotting is a technique used for the immunodetection of proteins and can be used for the quantification of proteins from complex protein mixtures [86]. With this technique, proteins separated by polyacrylamide gel electrophoresis are transferred onto an absorbent membrane thereby enable the detection and characterization of various proteins of interest using commercially available recombinant antibodies (Figure 2.7). Therefore, to determine the expression of the key receptor involved in promoting the formation of vasculogenic mimicry, VEGFR-1, the western blot technique was used.

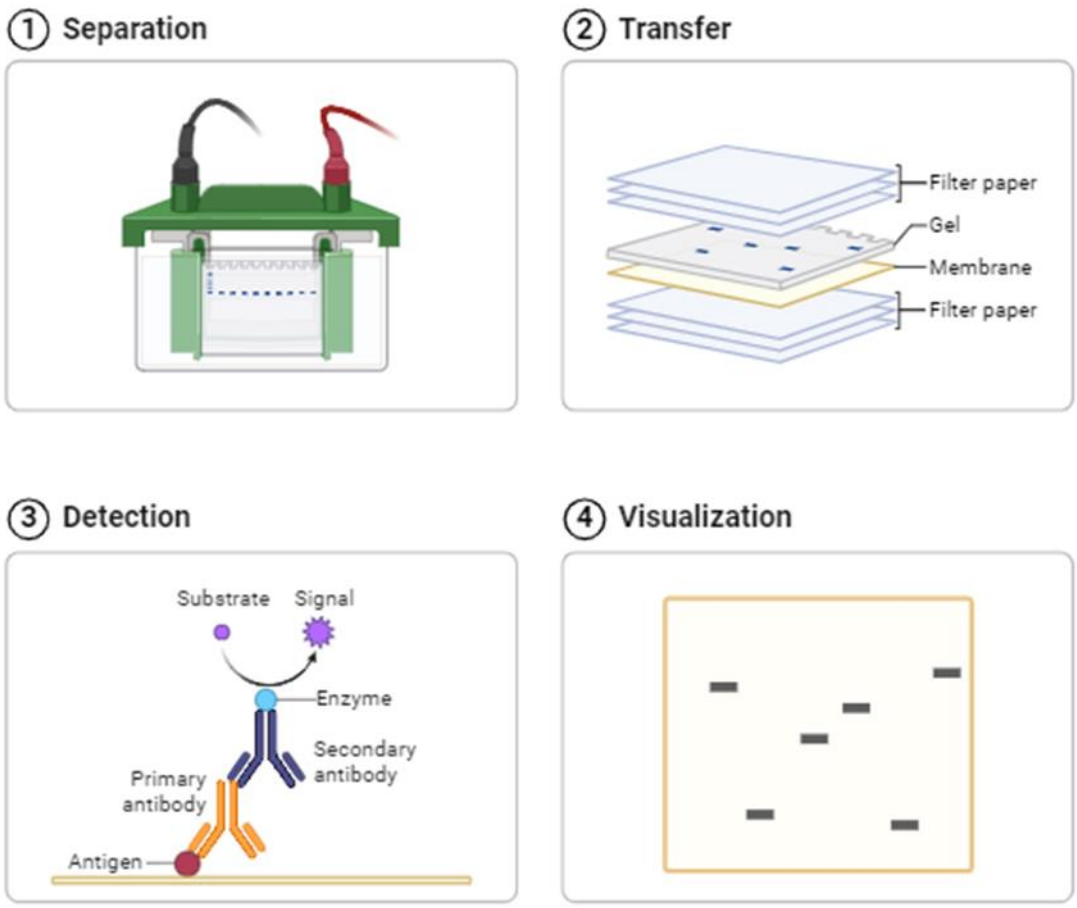

Figure 2.7 A graphical abstract illustrating the basic workflow of the western blot technique. (1) demonstrates protein separation by electrophoresis, (2) demonstrates the transfer of protein from SDS gel to a membrane, (3) illustrates immunodetection step using a primary antibody for antigen of interest and, (4) indicates the visualization step.

2.10.1 Cell lysate preparation

Melanoma B16-F10 cells were seeded in T25 cell culture flasks at a density of 500 000 cells per flask and allowed to attach overnight in a humidified atmosphere containing 5% CO_2 at 37 °C. The cells were exposed to sunitinib malate at an IC50 dose (2.6 µg/mL), double the IC50 dose (5.2 µg/mL) or in complete medium (DMEM) and re-incubated for 24 h following treatment exposure. Thereafter, the medium was removed and centrifuged at 2000 rpm for 5 min to retain any floating cells. Attached cells were washed twice with pre-warmed PBS and then treated with pre-warmed trypsin to enable detachment from the flasks. Thereafter, the mixture was transferred

to a 15 mL centrifuge tube (Thermo Scientific, Johannesburg, South Africa) and centrifuged at 2000 rpm for 5 min at RT. After centrifugation, the supernatant was discarded, and the cells were washed twice with ice-cold PBS before being lysed with radioimmunoprecipitation assay (RIPA) buffer (Sigma-Aldrich, St. Louis, MO, United States of America) containing Halt protease and phosphatase inhibitor cocktail (Thermo Scientific, Johannesburg, South Africa) and 0.5 mM EDTA on ice for 5 min. Thereafter, the lysate was centrifuged at 5000 rpm for 15 min to pellet the cell debris. The supernatant was then transferred to a new microcentrifuge tube (Sigma-Aldrich, St. Louis, MO, United States of America) and stored at -20 °C until needed.

2.10.2 Protein quantification

To determine the protein concentration of the prepared lysates, the bicinchoninic acid assay was used. With this technique, the stable water-soluble bicinchoninic acid, sodium salt tracks the production of cuprous ions (Cu^{+}) in protein reactions with alkaline Cu^{2+} by forming a deep purple colour which is stable and increases in intensity with an increase in protein concentration [87]. The cell lysates were thawed at RT prior use and added to each well of a 96-well plate (Thermo Scientific, Johannesburg, South Africa) alongside Bovine serum albumin (BSA) standards in triplicate. Thereafter, a standard working reagent prepared with 50 parts of Reagent A (sodium bicinchoninate (BCA), sodium carbonate (Na2CO3), sodium tartrate, sodium hydroxide (NaOH) and sodium bicarbonate (NaHCO3)) and 1 part of Reagent B (cupric sulphate (CuSO4)) was added to each well containing either the cell lysate or BSA standard. The 96-well plate was then covered with aluminium foil and placed on a shaker for 30 seconds to gently mix the contents and then incubated in an oven at 37 °C for 30 min. Thereafter, the plate was allowed to cool at RT before measuring the absorbance at 562 nm with and ELx 800 Universal Microplate reader (BioTek instruments Inc, Weltevreden, South Africa).

2.10.3 Protein separation and immunodetection

Following protein quantification, 20 µg of each cell lysate were loaded in sample buffer containing 1% β-mercaptoethanol and loaded onto a 12% polyacrylamide gel

alongside a protein ladder and separated at 60V for 15 min where after the voltage was increased to 120V for approximately 40 min in 1x gel running buffer (25 mM Tris, 190 mM Glycine and 0.1% SDS). Thereafter, proteins were electro-transferred using the Bio-Rad rapid transfer system (Bio-Rad, Hercules, CA, USA) onto nitrocellulose membranes at 2.5 A for 7 min. The membranes were then blocked with Tris-buffered saline-Tween (TBST) containing 3% BSA powder for 1 h at RT. Thereafter, the membranes were washed twice with TBST and incubated overnight at 4 °C with anti-VEGFR-1 (50 µg/mL) primary antibody (Sigma-Aldrich, St. Louis, MO, United States of America) diluted in TBST supplemented with 3% BSA. Monoclonal anti-actin was used as the housekeeping gene. Thereafter, membranes were washed once with TBST and incubated with a secondary antibody conjugated to Horseradish Peroxidase (HRP) for 1 h at RT with agitation. Membranes were washed three times for 10 min each with TBST at RT. Protein bands were visualised with ECL substrate and imaged using Chemidoc MP (Bio-Rad, Hercules, CA, USA) instrument.

2.11 Ethical Consent

Ethical clearance (655/2020) was obtained from the Research Ethics Committee, Faculty of Health Science at the University of Pretoria before commencing with the study (See Appendix II).

2.12 Data Analysis

The *in vivo* data for a sample size of eleven patients were analysed qualitatively in consultation with a pathologist. For the analysis of data from cell growth and migration measurements, a one-way analysis of variance (ANOVA) was used. For skewed data, nonparametric regression was employed. A sample size of nine was employed for analysis of cell growth and migration measurements. Statistical testing was at the 0.05 level of significance.

CHAPTER 3: RESULTS

3.1 Patient studies

The samples utilised for patient studies were obtained from patients diagnosed with melanoma with permission from the Department of Anatomical Pathology at the University of Pretoria, Pretoria, South Africa.

3.1.1 VEGF-A Immunohistochemistry

Vascular endothelial growth factor-A (VEGF-A) binds to VEGFR-1 to promote VM. To determine whether VEGF-A was expressed in melanoma biopsies, paraffin-embedded tumour sections from confirmed melanoma cases were immunohistochemically stained with anti-VEGF-A antibody. Since melanoma tissue has a natural melanin pigmentation, the chromogen used for detection was the Roche ultraView Universal Alkaline Phosphatase Red Detection kit to enable differentiation of protein of interest to the melanin in the tissue. The expression of VEGF-A was found in multiple hotspots intratumorally (Figure 3.1 A). Furthermore, results showed strong staining intensity (Figure 3.1 B)

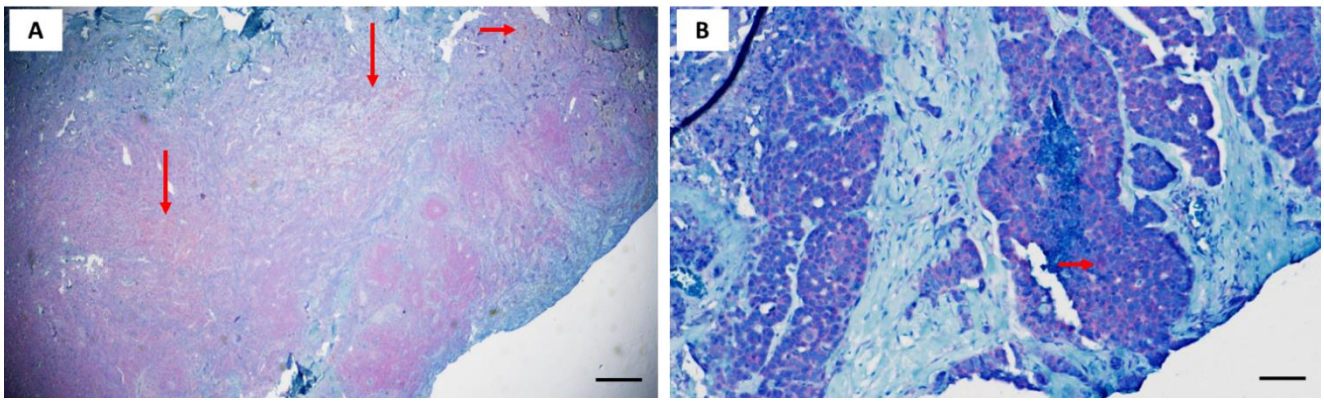

Figure 3.1 Representative images of VEGF-A staining in melanoma tissue by immunohistochemistry. (A), VEGF-A staining in multiple hotspots indicated by the red arrows (2x magnification, scale bar at 500 µm). (B), VEGF-A strong intensity staining (10x magnification, scale bar at 200 µm).

3.1.2 VCAM-1 Immunohistochemistry

Vascular cell adhesion molecule-1 (VCAM-1) is an adhesion molecule expressed on endothelial cells and plays a crucial role in leukocyte-endothelial cell interactions. Its upregulation is crucial for endothelial cell functions such as migration and tube formation, which are essential for forming the vessel-like structures seen in vasculogenic mimicry [88]. To determine whether VCAM-1 was expressed in melanoma biopsies, paraffin-embedded tumour sections from confirmed melanoma cases were immunohistochemically stained with anti-VCAM-1 antibody.

The expression of VCAM expression was found in multiple hotspots intratumorally and showed strong staining intensity (Figure 3.2 A,B).

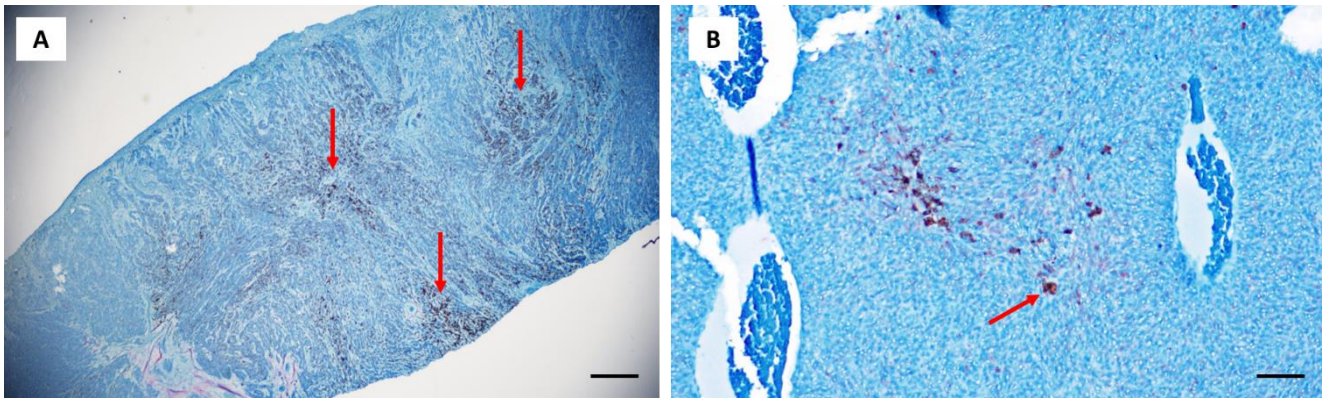

Figure 3.2 Representative images of VCAM1 staining in melanoma tissue by immunohistochemistry. (A), VCAM-1 staining in multiple hotspots indicated by the red arrows (2x magnification, scale bar at 500 µm). (B), VCAM-1 indication of strong staining intensity (10x magnification, scale bar at 200 µm).

3.1.3 Immunoreactivity scoring

To assess and score the expression of VEGF-A and VCAM-1, a modified Allred score, which is a combination of two parameters including proportion and intensity scores, was utilised. The expression of VEGF-A was observed in eight of the eleven evaluated samples. The expression of VCAM-1 was observed in four of the eleven evaluated patient samples (Figure 3.3).

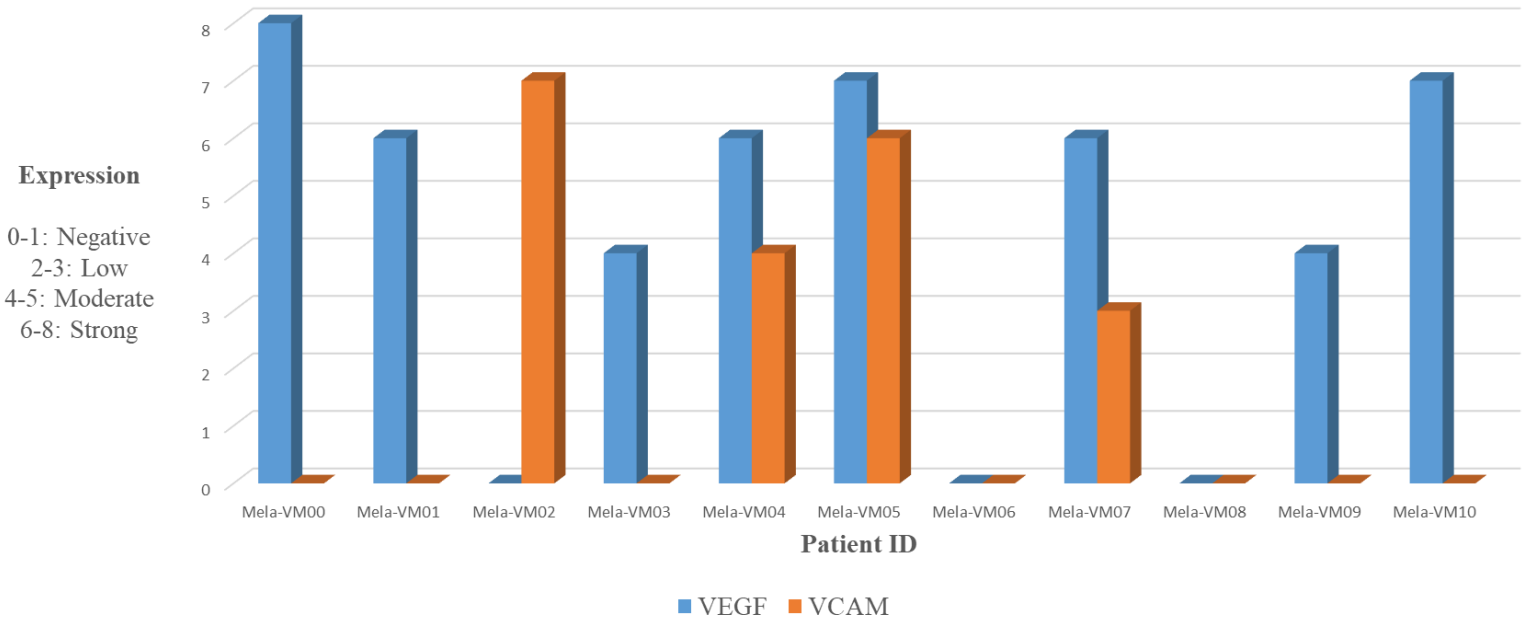

Figure 3.3 Immunoreactivity scoring for the expression of VEGF-A and VCAM-1 in melanoma tissue samples. Y-axis depicts the expression score of VEGF-A and VCAM-1 using a modified Allred score.

3.2 *In vitro* investigation results

Initially, the western blot technique was undertaken to determine the expression of the key receptor implicated in facilitating the development of VM, VEGFR-1 in the melanoma cell line employed in this study. The results showed that the cell line expressed the receptor, and the results are described under section 3.2.5. Further studies focused on the inhibition of the receptor and the effects of such inhibition on parameters associated with VM. The findings are discussed below.

3.2.1 Cell viability

Cell viability was determined using the crystal violet assay, which is cost-effective and simple.

The effect of sunitinib malate on the growth of the melanoma cell line, B16-F10 was evaluated over 24- and 48 hours. The results showed a dose-dependent decrease in cell viability after 24 hours for sunitinib treated samples (Figure 3.4 A).

B16-F10 cells treated with 0.1 µg/mL of sunitinib malate showed a moderate reduction in cell viability compared to the control. Treatment with 1 µg/mL sunitinib malate resulted in a moderate decrease in cell viability, while cells exposed to 10 µg/mL showed a markedly pronounced reduction in viability.

Similarly, sunitinib malate treated B16-F10 cells showed a significant dose-dependent decrease in viability compared to control after 48 hours of exposure (Figure 3.4 B). At 0.1 µg/mL sunitinib, the reduction in viability was moderate, while treatment with 1 µg/mL resulted in a significant decrease in viability. B16-F10 cells treated with 10 µg/mL also demonstrated a markedly significant reduction in viability compared to the control.

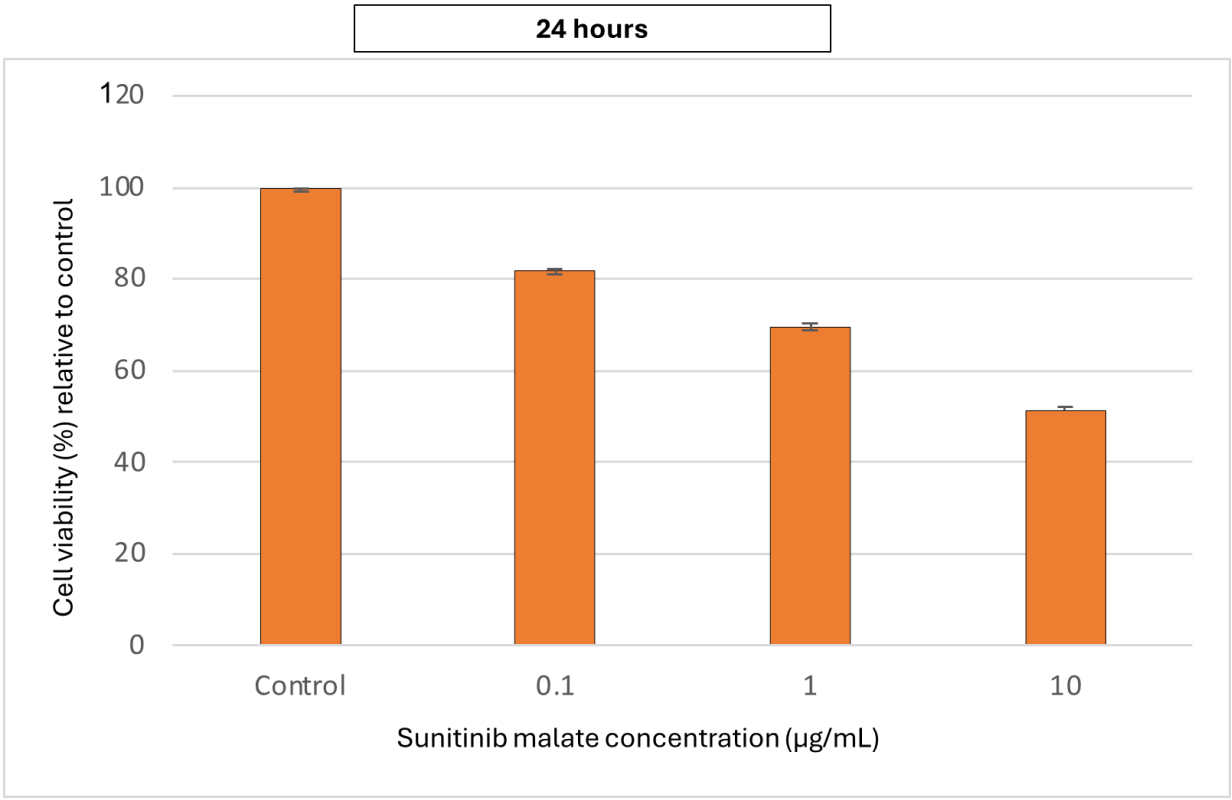

Figure 3.4 A The effect of sunitinib malate on B16-F10 cell viability after 24 hours of exposure. The cells were exposed to various concentrations (0.1 µg/mL, 1 µg/mL and 10 µg/mL) of sunitinib malate or no treatment for control cells. Results are represented as mean ±SD from three independent experiments.

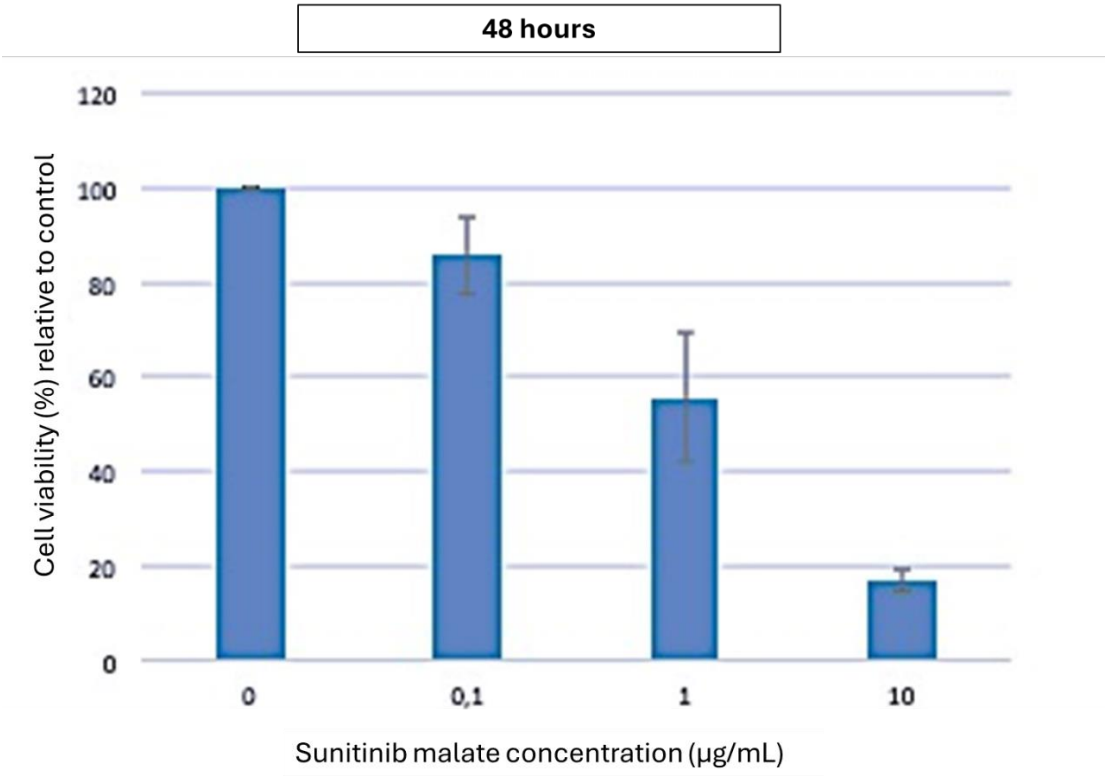

Figure 3.4 B The effect of sunitinib malate on B16-F10 cell viability after 48 hours of exposure. Results are represented as mean ±SD from three independent experiments. * indicates $p < 0.05$ compared to control.

In summary, sunitinib malate reduced the viability of B16-F10 melanoma cells in a dose-dependent manner. Low concentrations caused minimal growth inhibition, while higher concentrations led to a significant reduction in viability at 24 and 48 h.

Therefore, to gain insights into structural changes, attachment behaviour, and signs of apoptosis or cellular stress under treatment with sunitinib malate, morphological studies were conducted.

3.2.2 Morphological studies

Polarisation-optical interference (PlasDIC) microscopy was used to study the effects of sunitinib malate at the IC50 dose (2.6 µg/mL) and double IC50 (5.2 µg/mL) on the morphology of melanoma B16-F10 cells at 0 and 24 hours. Positive control cells were treated with physiological saline in culture medium.

When comparing control (Figure 3.5 A) and treated cells (Figure 3.5 B and C) at 0 hours, there are no significant differences in the morphology of cells. However, at 24 hours, cells treated with sunitinib malate 2.6 µg/mL (Figure 3.5 E), and 5.2 µg/mL (Figure 3.5 F) showed noticeable morphological changes compared to control cells. Of note is that cell rounding, membrane blebbing (Figure 3.5 E) and reduction in cell density were observed in sunitinib malate treated cells compared to control after 24 hours of exposure. These morphological changes indicate disruptions to the cytoskeleton, leading to hallmark features of apoptosis manifested as cell rounding and membrane blebbing and consequently reduced cell proliferation and death as observed in areas with reduced cell density (Figure 3.5 F). And, suggesting that treatment with sunitinib malate is inducing apoptosis in the cells and further confirms the inhibitory effects of sunitinib malate on melanoma cell growth.

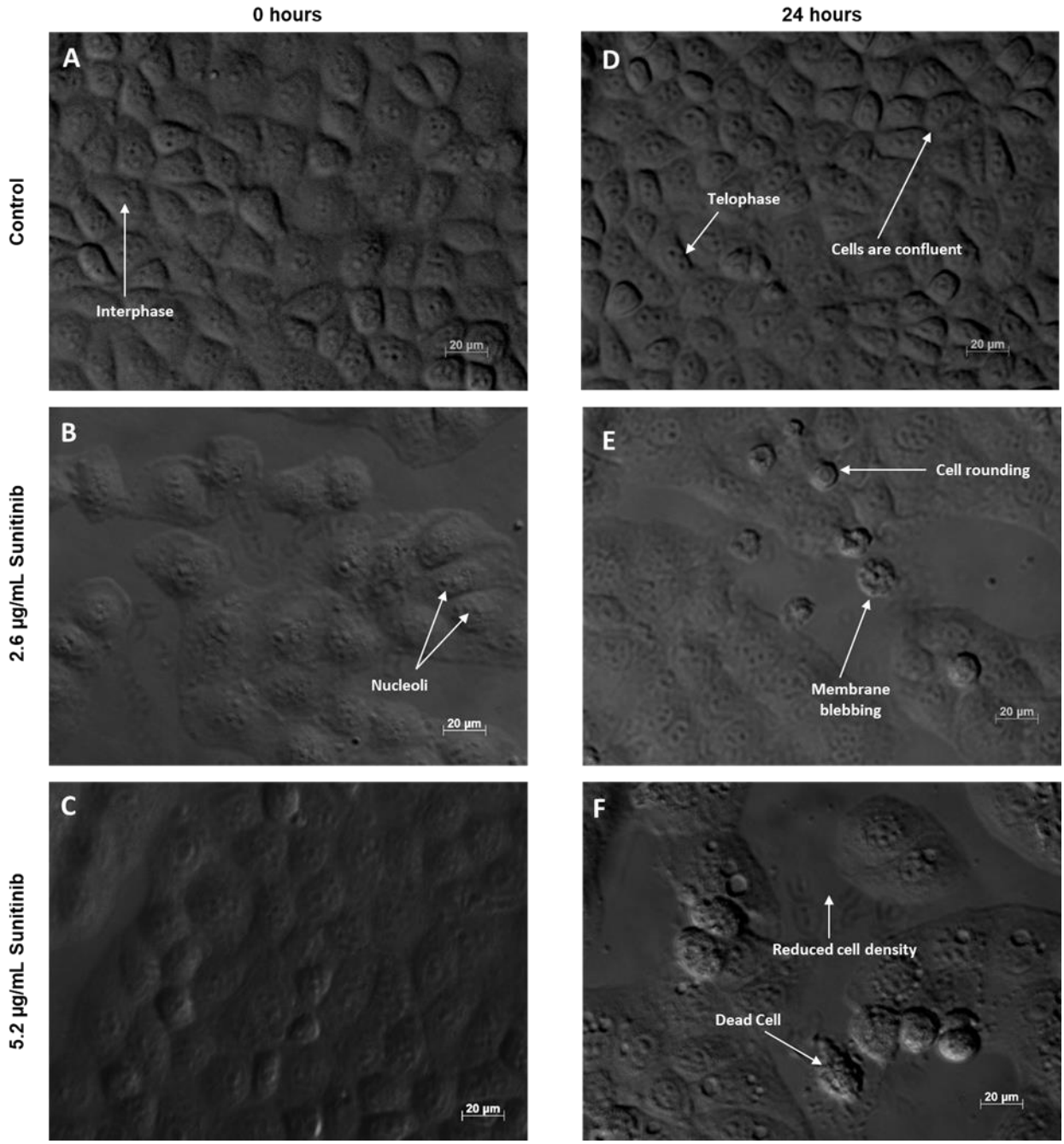

Figure 3.5 PlasDIC morphology images of melanoma cells at 0 hours **(A)** untreated cells (control), **(B)** sunitinib malate 2.6 µg/mL treated cells and **(C)** sunitinib malate 5.2 µg/mL treated cells. At 24 hours **(D)** untreated cells (control), **(E)** sunitinib malate 2.6 µg/mL treated cells and (F) sunitinib malate 5.2 µg/mL treated cells.

Following the observation of significant morphological changes such as cell rounding, membrane blebbing, and reduced cell density, it became imperative to further investigate the functional consequences of VEGFR-1 blockade using sunitinib malate

on cell migration, a critical feature in the progression of vasculogenic mimicry and metastasis.

3.2.3 *In vitro* scratch assay

The *in vitro* scratch assay was utilised to study the effects of sunitinib malate IC50 dose (2.6 µg/mL) and double IC50 dose (5.2 µg/mL) on the migration of melanoma cells over 22 hours. Migration was measured at 0, 6, 12 and 22 hours (Figure 3.6).

At 0 hours:

The wound area was comparable between the control and sunitinib malate-treated cells with both showing clearly defined edges and no initial migration into the wound area.

At 6 hours:

Control cells were showing signs of migration towards the wound area, whereas cells treated with sunitinib malate at IC50 dose did not show migration towards the wound area. Similarly, cells treated with sunitinib malate at double IC50 did not show migration into the wound area when compared to control cells.

At 12 hours:

The control cells continued migration into the wound area, progressing toward closure, whereas cells treated with sunitinib malate at IC50 showed minimal growth towards the wound area. In contrast, cells treated with sunitinib malate at double IC50 dose showed an increase in the wound width, indicating potential cell detachment or inhibition of migration.

At 22 hours:

Control cells showed substantial growth into the wound area, demonstrated by the significant decrease in wound width. Cells treated with sunitinib malate at IC50 dose showed some slight migration towards the wound area, though less pronounced compared to the control. In contrast, cells that were exposed to double IC50 dose of sunitinib malate continued to show an increase in wound width compared to control, suggesting a strong inhibitory effect on migration and possibly cell survival.

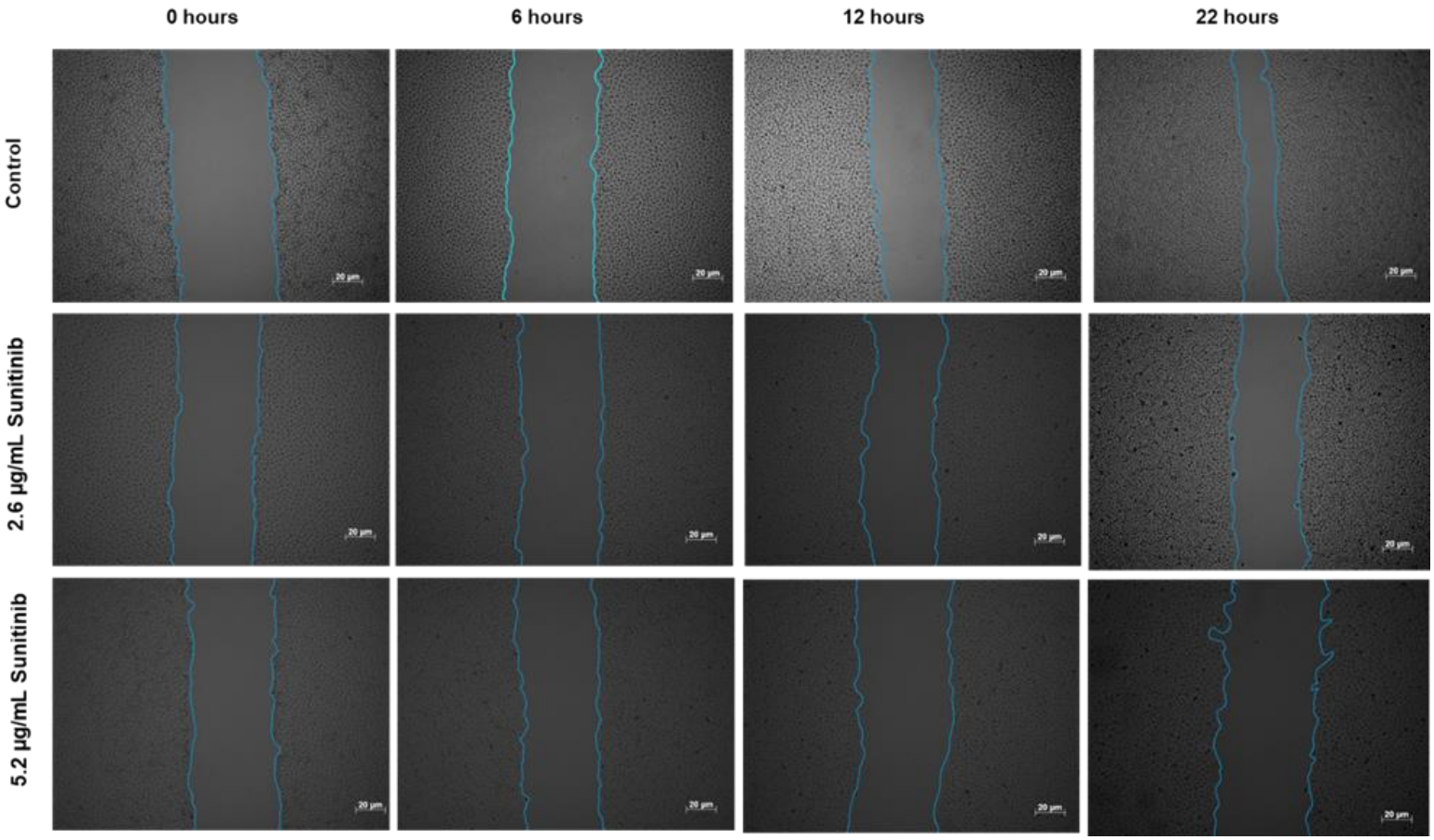

Figure 3.6 Representative *in vitro* scratch assay images of three biological repeats showing migration of melanoma cells over 22 hours. Melanoma cells were grown in cell culture plates and allowed to form a monolayer overnight. Once confluent, a "wound" was created using a 20 µl pipette tip. Images of the "wound" area were captured at 0, 6, 12 and 22 hours after exposure to sunitinib malate, whereby treated B16-F10 cells did not show migration into the wound area after 6 hours. Scale bar, 20 µm.

The wound width area was analysed quantitatively using ImageJ software and Graphpad prism version 10.1.2. for both control and sunitinib malate-treated cells.

At 0 hours, there were no significant difference in the wound width between control cells and cells treated with sunitinib malate (Figure 3.7), indicating uniform scratch creation across all groups. Similarly, at 6 hours, the wound width remained comparable between control and treated cells with no significant differences observed.

At 12 hours, the wound width for control cells was numerically smaller than that of cells treated with sunitinib malate at IC50 dose, though the difference was not statistically significant. However, there was a significant increase in the wound width for cells treated with sunitinib malate at double IC50 dose compared to control, indicating a dose-dependent inhibition of migration.

By 22 hours, significant differences in wound width were evident. The control cells showed a substantial decrease in wound width, whereas cells treated with sunitinib malate at IC50 dose showed significantly larger wound width, and similarly for cells treated with sunitinib malate at double IC50 showed a significantly larger wound width compared to control cells, further highlighting the inhibitory effect of sunitinib malate on melanoma cell migration in a dose-dependent manner.

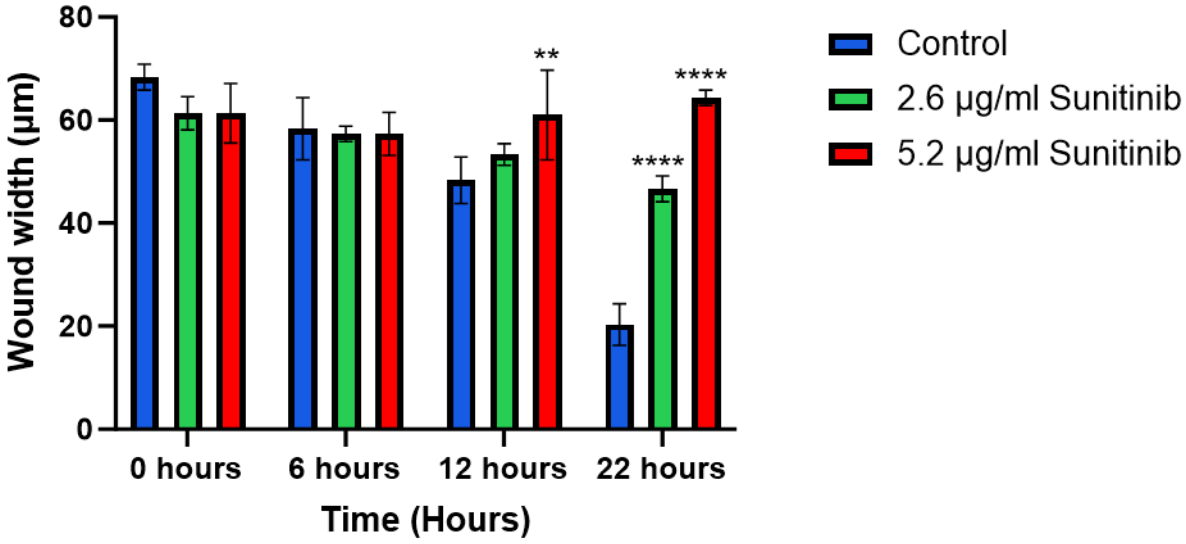

Figure 3.7 Sunitinib malate inhibits migration of melanoma cells. Quantitative analysis of melanoma cell migration over 22 hours after exposure to sunitinib malate. Values are expressed as mean wound width (µm) ± SD. ** $p < 0.001$. **** $p < 0.0001$ compared to control. Experiments were repeated three times.

3.2.4 Cell invasion and migration

The effect of sunitinib malate (VEGFR-1 inhibitor) on the growth of melanoma cells was monitored over 22 hours by measuring the electrical impedance using the xCELLigence system. Compared to the control (red), melanoma cells treated with

sunitinib malate at 0.1 µg/mL (green) showed a decrease in cell migration after 5 hours of exposure and reached a plateau phase from 8 hours of exposure until termination. Melanoma cells treated with 1 µg/mL of sunitinib malate (pink) showed a low cell index, indicating initial attachment without growth for up to 12 hours, after which the cell index progressively declined, suggesting reduced viability compared to the control. Similarly, melanoma cells treated with 10 µg/mL of sunitinib malate (blue) showed a consistently low cell index, indicative of attachment without growth compared to control **(Figure 3.8)**.

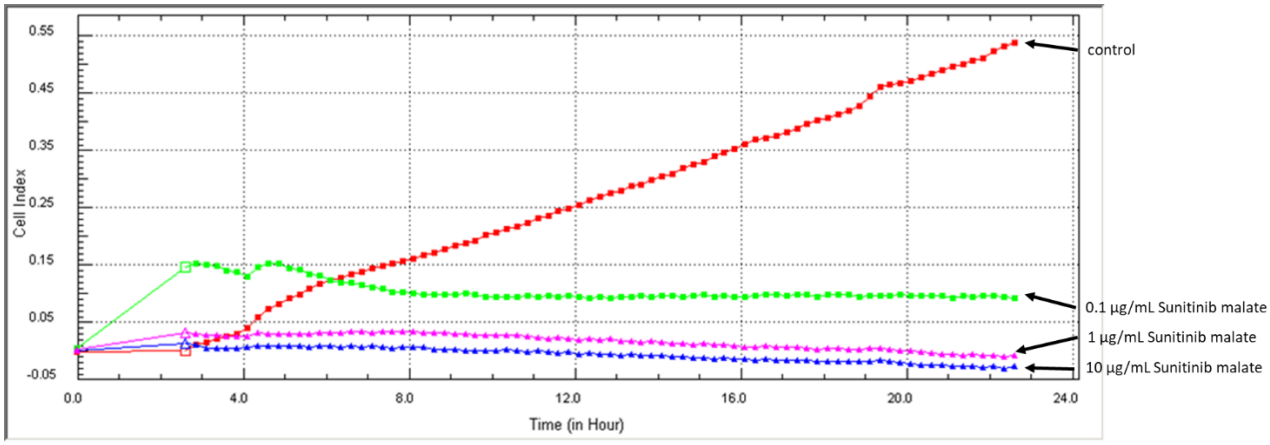

Figure 3.8 The effect of sunitinib malate on invasion and migration of melanoma cells over 22 hours. Cell index values are expressed as the mean of 4 wells. The red line indicates untreated cells (control), green, pink, and blue lines indicate growth of cells treated with 0.1, 1, and 10 µg/mL of sunitinib malate.

3.2.5 Western blotting

Western blot technique was utilised to determine the expression of the receptor which promotes vasculogenic mimicry, VEGFR-1 in the B16-F10 melanoma cell line.

The results showed that VEGFR-1 is expressed by the melanoma cell line B16-F10 (Figure 3.9). The effect of sunitinib malate on the expression level of this receptor.

There were no observable changes in the expression of VEGFR-1 for cells treated with sunitinib malate at 2.6 µg/ml compared to the control. Similarly, for melanoma cells treated with 5.2 µg/ml, there was no change when compared to the control.

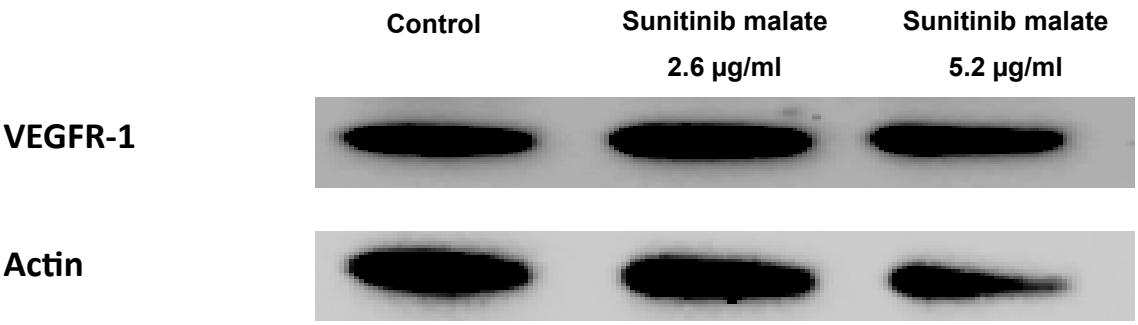

Figure 3.9 The effect of sunitinib malate on the expression of the key receptor implicated in the development of vasculogenic mimicry, VEGFR-1 in the B16-F10 melanoma cell line. Actin was used as the housekeeping gene. B16-F10 cells treated with sunitinib malate at a dose of 2.6 µg/mL and 5.2 µg/mL resulted in no change of expression levels of VEGFR-1 when compared to control.

CHAPTER 4: DISCUSSION

The formation of new blood vessels through VEGF-A induced angiogenesis is a pivotal process in melanoma growth, and metastasis [89]. Anti-angiogenic therapy, aimed at reducing tumour blood supply, has shown promising initial results in decreasing tumour size [90]. However, emerging evidence suggests that these therapies may also contribute to the transition of tumours to more aggressive growth phases [91]. This paradoxical effect highlights a critical challenge in the efficacy and use of anti-angiogenic treatments.

The *de novo* formation of microvasculature by tumour cells without the involvement of endothelial cells, vasculogenic mimicry [39] acts as an alternative tumour perfusion mechanism and thereby contribute to tumour progression and potential for metastasis. Notably, aggressive melanoma develops VM in response to hypoxia, and this phenomenon is observed following the use of anti-angiogenics such as bevacizumab. Furthermore, in melanoma, over 65% of the blood supply is implemented through VM channels [92]. However, *in vitro* studies evaluating the effect of anti-angiogenics on VM formation have shown that these drugs do not block the formation of vessel-like structures by tumour cells when compared to endothelial cell-lined vessels [71, 93]. In melanoma, VEGF-A drives VM by binding to VEGFR-1. This process is mediated through the activation of the PI3K/PKCα signalling pathway downstream of VEGFR-1, working in conjunction with integrin-mediated signalling to facilitate the formation of vessel-like structures [54].

Indeed, gene silencing of VEGFR-1 using cell lines (Mel Kor, Mel Cher, and Mel P) from surgical specimens of patients with disseminated melanoma resulted in disruption of capillary-like structures considered to be an *in-vitro* reconstitution of VM [54]. Furthermore, Frank and colleagues (2011) demonstrated the critical role of VEGFR-1 in malignant melanoma-initiating cells identified by the expression of the ATP-binding cassette (ABC) member ABCB5 whereby *in vivo* melanoma-specific short hairpin RNA mediated knockdown of VEGFR-1, blocked the development of VM morphology [94]. Additionally, VEGFR-1 blockade using a monoclonal antibody, D16F7, in a murine melanoma model demonstrated significant down regulation of the number of tube-like structures formed by melanoma cells upon exposure to VEGF-A [95]. Taken together,

these findings demonstrate the critical role of VEGFR-1 in melanoma progression and development of VM.

In this study, the presence of VM was investigated by evaluating the expression of proteins involved in VM signalling in melanoma tissue. The study also investigated the potential for VM by evaluating the effect of VEGFR-1 blockade on the growth patterns of the endothelioma cell line, sEnd.2 and aggressive melanoma cell line, B16-F10, as well as the effect of VEGFR-1 blockade on morphology, and migration of the aggressive melanoma cell line B16-F10.

4.1 Expression of VEGF-A

Immunohistochemistry was used to evaluate the expression of VEGF-A in melanoma tissue and its potential involvement in VM. The use of the Roche ultraview Universal Alkaline Phosphatase Red Detection kit was essential to distinguish protein expression from melanin pigmentation in melanoma tissues. This approach ensured accurate visualization of VEGF-A .

The results showed intratumoral expression of VEGF-A in multiple hotspots, demonstrating strong immunostaining intensity. Notably, the secretion of VEGF-A by melanoma cells has been established to play a key role in regulating angiogenesis, facilitating tumour vascularisation and growth [96]. Furthermore, there is evidence of VM formation when VEGF-A is bound to its receptor, VEGFR-1 in melanoma [97]. Therefore, the strong intratumoral expression of VEGF-A in melanoma biopsies underscores its potential involvement in VM, where tumour cells mimic endothelial cells to form vessel-like structures.

4.2 Expression of VCAM-1

Vascular cell adhesion molecule-1 (VCAM-1) is a member of the immunoglobulin superfamily of adhesion molecules and, plays a critical role in cell adhesion. It is a widely expressed protein, being found on macrophages, dendritic cells, epithelial cells, and on the surface of activated endothelial cells. Consequently, VCAM-1 may facilitate

tumour cell adhesion to vascular endothelial cells, thereby promoting the metastatic process [98].

The results from this study showed intratumoral expression of VCAM-1 in multiple hotspots, characterised by strong staining intensity. These findings align with previous research by Yong-Bin et al. (2003), which demonstrated that VCAM-1-positive tissues exhibit higher microvessel density than VCAM-1-negative tissues in gastric cancer [98]. Additionally, VCAM-1 expression has been closely associated with cancer metastasis. For instance, a comparative gene profile analysis revealed that upregulated VCAM-1 expression in metastatic breast cancer cells, particularly in parental MDA-MB-231 cells and in vivo isolates with lung metastatic activity [99]. Another study found that VCAM-1 is overexpressed in colorectal cancer and is associated with lymph node metastasis, clinical stage, and tumour progression in patients with colorectal cancer [100]. Therefore, these results highlight the critical role of VCAM-1 in tumour metastasis and progression, and further highlights its potential as a therapeutic target in cancer treatment.

In summary, immunohistochemistry results revealed the expression of VEGF-A and VCAM-1 in melanoma biopsies, indicating their involvement in VM. VEGF-A, a key angiogenic factor, upregulates VCAM-1, facilitating endothelial cell interactions and the formation of vessel-like structures (Figure 4.1) [88]. This interplay is crucial for providing tumours with blood supply, promoting melanoma progression and metastasis. Thus, targeting the VEGF-A/VCAM-1 pathway may offer a novel therapeutic approach to inhibit vasculogenic mimicry and tumour growth.

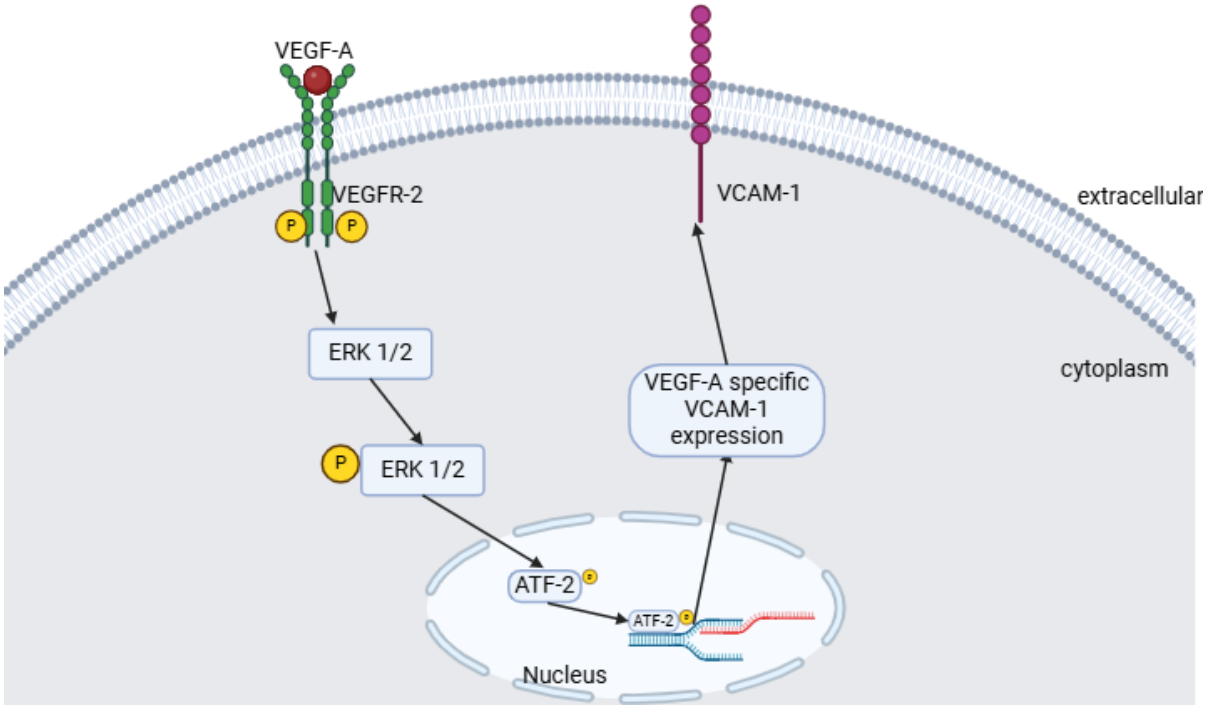

Figure 4.1 Schematic describing VEGF-A stimulation of intracellular signalling and activating transcription factor-2 (ATF-2)- regulated VCAM-1 gene expression. Adapted from Fearnly et al [88]

To further investigate the molecular mechanisms underlying VM, the next steps involved assessing the expression of VEGFR-1 in melanoma cells and the effect of VEGFR-1 blockade on the viability, proliferation, morphology, and migration of both benign tumour cells and aggressive melanoma cells.

To further understand the role of VEGFR-1 in melanoma and potential contribution to VM, cell viability and proliferation studies were conducted to evaluate the effects of VEGFR-1 blockade on these parameters.

4.3 Cell viability studies

The cost-effective and straightforward crystal violet assay was utilised, to evaluate the effect of sunitinib malate on cell viability for the aggressive melanoma cell line, B16-F10.

Crystal violet assay demonstrated a significant, dose-dependent decrease in the viability of aggressive melanoma cells after 24- and 48 hours of treatment with sunitinib malate. The progressive reduction in cell viability with increasing drug concentrations underscore the potent anti-proliferative effect of sunitinib malate on melanoma cells.

This finding aligns with evidence that endothelial cell proliferation is regulated by the binding of VEGF-A to its receptors, VEGFR-1 and VEGFR-2 [101]. However, the reduction in viability and growth in this study is likely attributed to the broad activity of sunitinib malate as a potent multi-targeted tyrosine kinase inhibitor with anti-tumour properties [102], which impacts both malignant and benign cells. Sunitinib malate has previously been correlated with the induction of apoptosis in endothelial cells and human umbilical vein cells *in vivo* and *in vitro* [103, 104]. Therefore, it is possible that the mode of action in affecting cell viability and proliferation at varying concentrations is through induction of apoptosis.

Notably, a significant reduction ($p < 0.05$) was observed exclusively in aggressive malignant cells, especially at sunitinib malate concentrations of 1 µg/mL and 10 µg/mL. These results indicate that sunitinib malate may be more potent against highly aggressive tumour cells, as demonstrated by the marked decrease in viability of B16-F10 melanoma cells. This highlights a differential cytotoxic effect, with more aggressive cells being more susceptible to treatment.

4.4 Morphological studies

Polarisation-optical interference (PlasDIC) microscopy was employed to investigate the morphological effects of sunitinib malate at IC50 (2.6 µg/mL) and double IC50 (5.2 µg/mL) concentrations on melanoma cells at 0 and 24 hours. The comparative analysis of control cells (Figure 3.6 A) and cells treated with sunitinib malate (Figures 3.6 B and C) at 0 hours showed no significant morphological differences.

However, at 24 hours, marked morphological changes were evident in cells treated with sunitinib malate at both 2.6 µg/mL (Figure 3.6 E) and 5.2 µg/mL (Figure 3.6 F) concentrations compared to control cells. Notable observations include cell rounding, membrane blebbing, and a reduction in cell density. These changes suggest significant cytoskeletal disruptions leading to apoptosis. The structural changes seen in treated cells are in line with typical cell death characteristics such as cell rounding, membrane blebbing and compromised cell density in culture [105].

Furthermore, the reduction in cell density observed in the treated cells implies a decrease in cell proliferation and an increase in cell death and validates the apoptotic effect of sunitinib malate.

Morphological observations of the B16-F10 melanoma cell line under distress align with findings from cell cycle analysis of the sEnd.2 endothelioma cell line treated with sunitinib malate by Scholtz and Mabeta[106]. The study reported a significant accumulation of cells in the Sub-G1 phase of the cell cycle, which is associated with cell death [106]. This suggests that the observed morphological alterations in aggressive melanoma cells, consistent with cell death, may be attributed to VEGFR-1 blockade.

While targeting VEGFR-1 has consistently been associated with decreased cell viability, reduced growth, and morphological characteristics indicative of cell death, recent findings by Rong et al [2] highlight the potential for resistance to such treatments. Specifically, significant morphological changes in sunitinib malate-resistant human microvascular endothelial cells (HMEC), which were linked to enhanced expression of efflux proteins that mitigate the effects of the drug [2] . Attempts to reverse resistance using fumitremorgin C (an ABC transporter inhibitor) or verapamil (a P-gp inhibitor) were unsuccessful, underscoring the complexity of overcoming drug resistance in these cells [2].

These findings suggest that while VEGFR-1 blockade can effectively delay cell cycle progression to the Sub-G1 phase, thereby reducing cell growth and migration *in vitro*, resistance mechanisms may ultimately limit its therapeutic efficacy. This highlights the importance of exploring combination strategies or additional targets to counteract resistance and enhance the benefits of VEGFR-1-targeted therapies.

4.5 Migration studies

A defining characteristic of malignant tumours is their ability to invade surrounding tissues and metastasize to distant organs. This involves several steps including detachment from the primary tumour, migration through connective tissues, intravasation into blood vessels, and colonization of distant sites [107, 108]. Melanoma is highly metastatic, driven by its efficient migration and ability to form a vascular network within tumour tissues. Notably, melanoma cells expressing VEGFR-1 are significantly more invasive than those lacking this receptor [109, 110]. Studies have demonstrated that blocking VEGFR-1 with specific monoclonal antibodies effectively reduces VEGF-A and placental growth factor (PlGF)-induced extracellular matrix invasion [111]. Another study utilised wound scratch assays whereby knock-down of VEGFR-1 in endothelial cells resulted in significantly impaired wound closure, with approximately 65% closure at 24 hours, further validating the role of VEGFR-1 in cell migration [112]. Recently, Koizumi *et al.* (2022) demonstrated that transfecting melanoma cells with VEGFR-1-targeting antisense oligonucleotides effectively suppressed VEGF-A induced cell migration [113]. These findings highlight the critical role of VEGFR-1 in promoting melanoma cell migration and invasion, providing a basis for exploring targeted therapies such as sunitinib malate as investigated in this study.

In this study, the *in vitro* scratch assay provided valuable insights into the inhibitory effects of sunitinib malate on melanoma cell migration in a dose- and time-dependent manner. Initially at 0 hours, the wound area was comparable between control and cells treated with sunitinib malate. At 6 hours, control cells began migrating into the wound area, while cells treated with sunitinib malate, even at the IC50 dose, showed no significant movement. This early inhibition suggests that sunitinib malate rapidly affects cellular mechanisms essential for migration. The lack of movement was even more pronounced in cells treated with the double IC50 dose, demonstrating a clear dose-dependent response.

By 12 hours, the migration of control cells continued, significantly reducing the wound width. In contrast, cells treated with sunitinib malate at the IC50 dose showed minimal movement, indicating partial inhibition of migration. Interestingly, cells treated with the double IC50 dose exhibited an increase in wound width, suggesting a potential

detachment of cells from the wound edge. This result suggests the cytotoxic effects or interference with cell adhesion mechanisms at higher drug concentrations over time.

At 22 hours, the inhibitory effects of sunitinib malate were more pronounced. Control cells demonstrated substantial closure of the wound, while cells treated with the IC50 dose showed limited migration toward the wound area. Cells treated with the double IC50 dose exhibited a further increase in wound width, highlighting a strong inhibitory effect on migration and potential cytotoxicity. Quantitative analysis confirmed significant differences in wound width, particularly between control and double IC50-treated groups, reinforcing the dose-dependent nature of sunitinib malate's effects.

These results, aligns with findings from the crystal violet assay, which revealed a significant, dose-dependent reduction in melanoma cell viability at 24 and 48 hours, highlighting sunitinib malate's potent anti-proliferative effects. Moreover, morphological changes such as cell rounding, membrane blebbing, and reduced cell density at 24 hours further support the notion of cytoskeletal disruption and apoptosis. Collectively, these findings suggest that sunitinib malate inhibits melanoma cell migration and proliferation while inducing cell death. This highlights its potential as a therapeutic agent against aggressive melanoma.

In addition, results obtained using the real-time label-free xCELLigence system revealed a dose-dependent decrease in cell invasion and migration over a 22-hour period, with the higher concentration (10 µg/mL) significantly inhibiting cell invasion and migration (Figure 3.10).

These results are consistent with findings by Li et al. (2014), which demonstrated that invasion and migration of melanoma cells expressing high levels of VEGFR-1 could be inhibited by ranibizumab through VEGF antagonism at VEGFR-1[114].

Moreover, these results are also align with studies on non-transformed human umbilical vein endothelial cells (HUVECs), where sunitinib malate significantly inhibited cell migration within 9 hours [115]. Similarly, sunitinib malate at a 5 µM dose has been shown to inhibit the migration of both benign and malignant meningioma cells [116]

These findings align with sunitinib malate's function as a multi-target tyrosine kinase inhibitor, which disrupts key signalling pathways such as VEGFR-1-PI3k/Akt and

platelet derived growth factor receptors (PDGFR) that regulate migration and adhesion[112, 113].

4.6 Western blot analysis

Vascular endothelial growth factor receptor-1 has been identified in various tumour cells, including melanoma, where its activation by autocrine or paracrine ligands plays a critical role in promoting cell survival, migration, and invasiveness [94, 95, 117, 118]. Notably, VEGFR-1 expression is significantly upregulated under conditions that induce VM, such as hypoxia [119, 120].

In this study, VEGFR-1 expression in the B16-F10 melanoma cell line was confirmed using the Western blot technique, further supporting its role in melanoma biology. Interestingly, treatment with sunitinib malate, at a dose of 2.6 µg/mL and 5.2 µg/mL did not alter VEGFR-1 expression levels compared to the untreated control. This suggests that VEGFR-1 may be regulated through mechanisms that are not directly affected by sunitinib malate. It is also possible that sunitinib malate might primarily influence VEGFR-1 activity rather than its expression.

CHAPTER 5: CONCLUSION

This study investigated the presence of VM *in vivo* and processes associated with VM *in vitro.* The expression of proteins known to promote VM, VEGF-A and VCAM-1 were investigated initially in melanoma tissues.

Immunohistochemistry revealed strong intratumoral expression of VEGF-A and VCAM-1 in melanoma tissues. VEGF-A was implicated in promoting angiogenesis and VM, while VCAM-1 was linked to enhancing metastatic potential through increased cell adhesion. Together, these findings suggest that VEGF-A and VCAM-1 operate via complementary pathways to support melanoma invasion and metastasis. Positive immunohistochemical staining for VEGF-A and VCAM-1 may offer valuable insights into the potential for VM, highlighting the importance of expanded diagnostic tests to assess for metastasis and early therapeutic intervention targeting VM pathways.

Due to challenges with optimising the western blot technique, it was decided to only use cultured cells, owing to the amount of time it had already taken, and not include tissue samples. The presence of VEGFR-1 in B16-F10 melanoma cells was established. Subsequently, molecular mechanisms implicated in VM were investigated *in vitro* by evaluating the effect of VEGFR-1 blockade using sunitinib malate on melanoma cell viability, morphology, and migration and invasion, as well as protein expression.

Western blot analysis confirmed VEGFR-1 expression in the B16-F10 melanoma cell line, reinforcing its role in melanoma biology. Notably, treatment with sunitinib malate at 2.6 µg/mL and 5.2 µg/mL did not alter VEGFR-1 expression levels, suggesting that the drug may primarily influence VEGFR-1 activity rather than its expression.

Crystal violet assays and real-time label free proliferation assay demonstrated the efficacy of sunitinib malate in inhibiting melanoma cell viability and proliferation in a dose-dependent manner. These findings confirm its potent anti-proliferative effects on aggressive melanoma cells, consistent with its role as a multi-targeted tyrosine kinase inhibitor disrupting VEGFR-1 signalling. The reduction in viability and growth observed in benign endothelioma cells further highlights sunitinib malate's broad activity.

Morphological analysis revealed hallmark signs of apoptosis, including cell rounding and membrane blebbing, which were consistent with cytoskeletal disruptions and cell

death. These changes, consistent with apoptotic cell death, were particularly pronounced at higher drug concentrations, corroborating the inhibitory effects on cell growth and adhesion mechanisms.

Migration studies using the *in vitro* scratch assay clearly demonstrated the potent inhibitory effects of sunitinib malate on melanoma cell migration. A clear dose- and time-dependent inhibition of migration was observed, whereby higher drug concentration not only attenuates migration but also leads to detachment from the wound edge, emphasizing its cytotoxic potential. These findings are consistent with previous studies demonstrating the anti-migratory effects of sunitinib malate across various cell types, including endothelial and meningioma cells.

While sunitinib malate inhibited various processes associated with VM, it had no observable effect on VEGFR-1 expression at the doses used. It may be important to test the drug in combination with potent VEGFR-1 targeting drugs such as D16F7.

Overall, this study reinforces the critical role of VEGFR-1 signalling in melanoma progression and highlights the therapeutic potential of sunitinib malate as a targeted treatment strategy. However, emerging evidence of resistance to VEGFR-1 targeted therapies underscores the necessity of exploring combination treatments or additional targets to overcome such limitations.

In conclusion, the results further contribute to the advances made in the understanding of VM in melanoma progression, while highlighting the therapeutic potential of targeting the VEGF-A/ VEGFR-1 pathway, as well as VCAM-1. Indeed, the findings of this study contribute to the foundation for developing more targeted and effective therapeutic strategies to disrupt vasculogenic mimicry and its associated enhancement of treatment resistance in melanoma.

5.1 FUTURE STUDIES

The limitation of this study was the small patient sample size. Future studies should include more patient samples and further focus on investigating additional VM

markers, such as VE-Cadherin or EphA2 to improve early detection of VM and enable better prediction of treatment responses. Functional assays, including tube formation or 3D culture systems, could complement the immunohistochemistry results and provide direct evidence of VM. Moreover, exploring the molecular pathways linking VEGF-A and VCAM-1 to VM in melanoma could uncover novel therapeutic targets. Additionally, investigating combination therapies such as sunitinib malate and D16F7, or agents targeting complementary pathways like VEGF-A and VCAM-1, could enhance therapeutic efficacy and address the challenge of drug resistance. Expanding the scope of *in vivo* studies using animal models will be crucial to validate the inhibitory effects of sunitinib malate on VM-related processes, such as angiogenesis, migration, and invasion, while assessing its impact on tumour progression and metastasis. Together, these focus areas will contribute to advancing therapeutic strategies and improving outcomes for melanoma patients.

References

1. Lai-Cheong JE, McGrath JA. Structure and function of skin, hair and nails. Medicine. 2017; 45(6):347-51. doi:10.1016/j.mpmed.2017.03.004
2. Zhang R, Huang L, Pan D, Zhang W. Sunitinib induced resistance of endothelial cells by up-regulating P-glycoprotein and PI3K/Akt pathway. Braz J Pharm. 2022; 58 doi:10.1590/s2175-97902022e191102
3. Losquadro WD. Anatomy of the Skin and the Pathogenesis of Nonmelanoma Skin Cancer. Facial Plast Surg Clin North Am. 2017; 25(3):283-9. doi:10.1016/j.fsc.2017.03.001
4. Wang JX, Fukunaga-Kalabis M, Herlyn M. Crosstalk in skin: melanocytes, keratinocytes, stem cells, and melanoma. J Cell Commun Signal. 2016; 10(3):191-6. doi:10.1007/s12079-016-0349-3
5. Arnette CR, Roth-Carter QR, Koetsier JL, Broussard JA, Burks HE, Cheng K, et al. Keratinocyte cadherin desmoglein 1 controls melanocyte behavior through paracrine signaling. Pigment Cell Melanoma Res. 2020; 33(2):305-17. doi:10.1111/pcmr.12826
6. Apalla Z, Lallas A, Sotiriou E, Lazaridou E, Ioannides D. Epidemiological trends in skin cancer. Dermatol Pract Concept. 2017; 7(2):1-6. doi:10.5826/dpc.0702a01
7. Wright CY, du Preez DJ, Millar DA, Norval M. The Epidemiology of Skin Cancer and Public Health Strategies for Its Prevention in Southern Africa. International Journal of Environmental Research and Public Health. 2020; 17(3):1017. doi:10.3390/ijerph17031017
8. Karimkhani C, Green AC, Nijsten T, Weinstock MA, Dellavalle RP, Naghavi M, Fitzmaurice C. The global burden of melanoma: results from the Global Burden of Disease Study 2015. Br J Dermatol. 2017; 177(1):134-40. doi:10.1111/bjd.15510
9. Linares MA, Zakaria A, Nizran P. Skin Cancer. Prim Care. 2015; 42(4):645-59. doi:10.1016/j.pop.2015.07.006
10. Fajuyigbe D, Lwin SM, Diffey BL, Baker R, Tobin DJ, Sarkany RPE, Young AR. Melanin distribution in human epidermis affords localized protection against DNA photodamage and concurs with skin cancer incidence difference in extreme phototypes. FASEB J. 2018; 32(7):3700-6. doi:10.1096/fj.201701472R
11. Arrangoiz R. Melanoma Review: Epidemiology, Risk Factors, Diagnosis and Staging. J Cancer Treat Res. 2016; 4(1) doi:10.11648/j.jctr.20160401.11
12. Zhang Z, Imani S, Shasaltaneh MD, Hosseinifard H, Zou L, Fan Y, Wen Q. The role of vascular mimicry as a biomarker in malignant melanoma: a systematic review and meta-analysis. BMC Cancer. 2019; 19(1):1134. doi:10.1186/s12885-019-6350-5
13. Elder DE. Melanoma progression. Pathology. 2016; 48(2):147-54. doi:10.1016/j.pathol.2015.12.002
14. Thompson JF, Scolyer RA, Kefford RF. Cutaneous melanoma. Lancet. 2005; 365(9460):687-701. doi:10.1016/s0140-6736(05)17951-3
15. Miller AJ, Mihm MC, Jr. Melanoma. NEJM. 2006; 355(1):51-65.
16. AICR/WCRF. World Cancer Research Fund International. World Cancer Research Fund International [Internet]. 2019 June 14. Available from: https://www.wcrf.org/sites/default/files/Skin-cancer.pdf.
17. The Global Cancer Observatory. The Global Cancer Observatory2019.
18. Scalvenzi M, Megna M, Costa C, Fabbrocini G, Villani A, Greco V. Cutaneous melanoma associated with naevi prevalence: A 15-year cross-sectional retrospective study. Australas J Dermatol. 2020; 61(1):39-42. doi:10.1111/ajd.13171
19. Gray-Schopfer V, Wellbrock C, Marais R. Melanoma biology and new targeted therapy. Nature. 2007; 445(7130):851-7. doi:10.1038/nature05661
20. Houghton AN, Polsky D. Focus on melanoma. Cancer Cell. 2002; 2(4):275-8.
21. Roja Ramani D, Ranjani SS. An Efficient Melanoma Diagnosis Approach Using Integrated HMF Multi-Atlas Map Based Segmentation. J Med Syst. 2019; 43(7):225. doi:10.1007/s10916-019-1315-4
22. Watts CG, Dieng M, Morton RL, Mann GJ, Menzies SW, Cust AE. Clinical practice guidelines for identification, screening and follow-up of individuals at high risk of primary cutaneous melanoma: a systematic review. Br J Dermatol. 2015; 172(1):33-47. doi:10.1111/bjd.13403

23. Yuxin Liu MSS. Melanoma: Molecular Pathogenesis and Therapeutic Management. Molecular and cellular pharmacology. 2014:228-.
24. Schadendorf D, van Akkooi ACJ, Berking C, Griewank KG, Gutzmer R, Hauschild A, et al. Melanoma. Lancet. 2018; 392(10151):971-84. doi:10.1016/s0140-6736(18)31559-9
25. Michielin O, van Akkooi ACJ, Ascierto PA, Dummer R, Keilholz U, clinicalguidelines@esmo.org EGCEa. Cutaneous melanoma: ESMO Clinical Practice Guidelines for diagnosis, treatment and follow-updagger. Ann Oncol. 2019; 30(12):1884-901. doi:10.1093/annonc/mdz411
26. Keung EZ, Gershenwald JE. The eighth edition American Joint Committee on Cancer (AJCC) melanoma staging system: implications for melanoma treatment and care. Expert Rev Anticancer Ther. 2018; 18(8):775-84. doi:10.1080/14737140.2018.1489246
27. Gershenwald JE, Scolyer RA. Melanoma Staging: American Joint Committee on Cancer (AJCC) 8th Edition and Beyond. Ann Surg Oncol. 2018; 25(8):2105-10. doi:10.1245/s10434-018-6513-7
28. Domingues B, Lopes JM, Soares P, Populo H. Melanoma treatment in review. Immunotargets Ther. 2018; 7:35-49. doi:10.2147/ITT.S134842
29. Davey RJ, van der Westhuizen A, Bowden NA. Metastatic melanoma treatment: Combining old and new therapies. Crit Rev Oncol Hematol. 2016; 98:242-53. doi:10.1016/j.critrevonc.2015.11.011
30. Prado G, Svoboda RM, Rigel DS. What's New in Melanoma. Dermatologic clinics. 2019; 37(2):159-68. doi:10.1016/j.det.2018.12.005
31. Gogas HJ, Kirkwood JM, Sondak VK. Chemotherapy for metastatic melanoma: time for a change? Cancer. 2007; 109(3):455-64. doi:10.1002/cncr.22427
32. Lugowska I, Teterycz P, Rutkowski P. Immunotherapy of melanoma. Contemp Oncol (Pozn). 2018; 22(1A):61-7. doi:10.5114/wo.2018.73889
33. Axel Hauschild J-JG, Lev V. Demidov, et al. Dabrafenib in BRAF-mutated metastatic melanoma: a multicentre, open-label, phase 3 randomised controlled trial. Lancet. 2012:358-65.
34. Amann VC, Ramelyte E, Thurneysen S, Pitocco R, Bentele-Jaberg N, Goldinger SM, et al. Developments in targeted therapy in melanoma. Eur J Surg Oncol. 2017; 43(3):581-93. doi:10.1016/j.ejso.2016.10.014
35. Kimberly A. Varker JEB, Cheryl Kefauver, et al. A Randomized Phase 2 Trial of Bevacizumab with or without Daily Low-Dose Inteferon Alfa-2b in Metastatic Malignant Melanoma. Annals of Surgical Oncology. 2007:2367-76.
36. Jour G, Ivan D, Aung PP. Angiogenesis in melanoma: an update with a focus on current targeted therapies. J Clin Pathol. 2016; 69(6):472-83. doi:10.1136/jclinpath-2015-203482
37. von Moos R, Seifert B, Simcock M, Goldinger SM, Gillessen S, Ochsenbein A, et al. First-line temozolomide combined with bevacizumab in metastatic melanoma: a multicentre phase II trial (SAKK 50/07). Ann Oncol. 2012; 23(2):531-6. doi:10.1093/annonc/mdr126
38. Pinto MP, Sotomayor P, Carrasco-Avino G, Corvalan AH, Owen GI. Escaping Antiangiogenic Therapy: Strategies Employed by Cancer Cells. Int J Mol Sci. 2016; 17(9) doi:10.3390/ijms17091489
39. Maniotis AJ, Folberg R, Hess A, Seftor EA, Gardner LM, Pe'er J, et al. Vascular channel formation by human melanoma cells in vivo and in vitro: vasculogenic mimicry. Am J Pathol. 1999; 155(3):739-52. doi:10.1016/s0002-9440(10)65173-5
40. Folberg R, Maniotis AJ. Vasculogenic mimicry. APMIS. 2004; 112(7-8):508-25. doi:10.1111/j.1600-0463.2004.apm11207-0810.x
41. Folberg R, Hendrix MJC, Maniotis AJ. Vasculogenic Mimicry and Tumor Angiogenesis. Am J Pathol. 2000; 156(2):361-81. doi:10.1016/S0002-9440(10)64739-6
42. Warso MA, Maniotis AJ, Chen X, Majumdar D, Patel MK, Shilkaitis A, et al. Prognostic significance of periodic acid-Schiff-positive patterns in primary cutaneous melanoma. Clinical cancer research : an official journal of the American Association for Cancer Research. 2001; 7(3):473-7.
43. Treps L, Faure S, Clere N. Vasculogenic mimicry, a complex and devious process favoring tumorigenesis - Interest in making it a therapeutic target. Pharmacol Ther. 2021:107805. doi:10.1016/j.pharmthera.2021.107805

44. Zhang X, Zhang J, Zhou H, Fan G, Li Q. Molecular Mechanisms and Anticancer Therapeutic Strategies in Vasculogenic Mimicry. J Cancer. 2019; 10(25):6327-40. doi:10.7150/jca.34171
45. Frenkel S, Barzel I, Levy J, Lin AY, Bartsch DU, Majumdar D, et al. Demonstrating circulation in vasculogenic mimicry patterns of uveal melanoma by confocal indocyanine green angiography. Eye (London, England). 2008; 22(7):948-52.
46. Hess AR, Seftor EA, Gardner LM, Carles-Kinch K, Schneider GB, Seftor RE, et al. Molecular regulation of tumor cell vasculogenic mimicry by tyrosine phosphorylation: role of epithelial cell kinase (Eck/EphA2). Cancer research. 2001; 61(8):3250-5.
47. Mary JCH, Lynn MGG, Richard EBS, Seftor EA, Meltzer PS, Hess AR, et al. Expression and Functional Significance of VE-Cadherin in Aggressive Human Melanoma Cells: Role in Vasculogenic Mimicry. Proceedings of the National Academy of Sciences of the United States of America. 2001; 98(14):8018-23.
48. Paulis YW, Soetekouw PM, Verheul HM, Tjan-Heijnen VC, Griffioen AW. Signalling pathways in vasculogenic mimicry. Biochim Biophys Acta. 2010; 1806(1):18-28. doi:10.1016/j.bbcan.2010.01.001
49. Delgado-Bellido D, Fernandez-Cortes M, Rodriguez MI, Serrano-Saenz S, Carracedo A, Garcia-Diaz A, Oliver FJ. VE-cadherin promotes vasculogenic mimicry by modulating kaiso-dependent gene expression. Cell Death Differ. 2019; 26(2):348-61. doi:10.1038/s41418-018-0125-4
50. Kirschmann DA, Seftor EA, Hardy KM, Seftor RE, Hendrix MJ. Molecular pathways: vasculogenic mimicry in tumor cells: diagnostic and therapeutic implications. Clin Cancer Res. 2012; 18(10):2726-32. doi:10.1158/1078-0432.CCR-11-3237
51. Hess AR, Seftor EA, Gruman LM, Kinch MS, Seftor RE, Hendrix MJ. VE-cadherin regulates EphA2 in aggressive melanoma cells through a novel signaling pathway: implications for vasculogenic mimicry. Cancer Biol Ther. 2006; 5(2):228-33. doi:10.4161/cbt.5.2.2510
52. Mabeta P. Paradigms of vascularization in melanoma: Clinical significance and potential for therapeutic targeting. Biomed Pharmacother. 2020; 127:110135. doi:https://doi.org/10.1016/j.biopha.2020.110135
53. Mary J. Hendrix EAS, Angela R. Hess, Richard E. Seftor. Vasculogenic mimicry and tumor-cell plasticity: Lessons from melanoma. Nature 2003:411-21.
54. Vartanian A, Stepanova E, Grigorieva I, Solomko E, Baryshnikov A, Lichinitser M. VEGFR1 and PKCalpha signaling control melanoma vasculogenic mimicry in a VEGFR2 kinase-independent manner. Melanoma Res. 2011; 21(2):91-8. doi:10.1097/CMR.0b013e328343a237
55. Xu X, Zong Y, Luo W, Jia S, Gao Y, Sun X, Zhao H. VEGF Induce Vasculogenic Mimicry of Choroidal Melanoma through the PI3k Signal Pathway. Biomed Res Int. 2019; 2019 doi:10.1155/2019/3909102
56. Quail DF, Taylor MJ, Walsh LA, Dieters-Castator D, Das P, Jewer M, et al. Low oxygen levels induce the expression of the embryonic morphogen Nodal. Mol Biol Cell. 2011; 22(24):4809-21. doi:10.1091/mbc.E11-03-0263
57. Postovit LM, Margaryan NV, Seftor EA, Hendrix MJ. Role of nodal signaling and the microenvironment underlying melanoma plasticity. Pigment Cell Melanoma Res. 2008; 21(3):348-57. doi:10.1111/j.1755-148X.2008.00463.x
58. Topczewska JM, Postovit LM, Margaryan NV, Sam A, Hess AR, Wheaton WW, et al. Embryonic and tumorigenic pathways converge via Nodal signaling: role in melanoma aggressiveness. Nat Med. 2006; 12(8):925-32. doi:10.1038/nm1448
59. McAllister JC, Zhan Q, Weishaupt C, Hsu M-Y, Murphy GF. The embryonic morphogen, Nodal, is associated with channel-like structures in human malignant melanoma xenografts. Journal of Cutaneous Pathology. 2010; 37(s1):19-25.
60. Strizzi L, Postovit L-M, Margaryan NV, Lipavsky A, Gadiot J, Blank C, et al. Nodal as a biomarker for melanoma progression and a new therapeutic target for clinical intervention. Expert Rev Dermatol. 2009; 4(1):67-78. doi:10.1586/17469872.4.1.67
61. Thies A, Mangold U, Moll I, Schumacher U. PAS-positive loops and networks as a prognostic indicator in cutaneous malignant melanoma. The Journal of Pathology. 2001; 195(5):537-42. doi:10.1002/path.988

62. van Beurden A, Schmitz RF, van Dijk CM, Baeten CI. Periodic acid Schiff loops and blood lakes associated with metastasis in cutaneous melanoma. Melanoma research. 2012; 22(6):424-9. doi:10.1097/CMR.0b013e328358b355
63. Spiliopoulos K, Peschos D, Batistatou A, Ntountas I, Papoudou-Bai A, Zioga A, et al. Immunohistochemical Study of Vasculogenic Mimicry and Angiogenesis in Melanocytic Tumors of the Eye and the Periocular Area. Anticancer Res. 2017; 37(3):1113-20. doi:10.21873/anticanres.11424
64. Yang JP, Liao YD, Mai DM, Xie P, Qiang YY, Zheng LS, et al. Tumor vasculogenic mimicry predicts poor prognosis in cancer patients: a meta-analysis. Angiogenesis. 2016; 19(2):191-200. doi:10.1007/s10456-016-9500-2
65. Ge H, Luo H. Overview of advances in vasculogenic mimicry - a potential target for tumor therapy. Cancer Manag Res. 2018; 10:2429-37. doi:10.2147/CMAR.S164675
66. Baeten CI, Hillen F, Pauwels P, de Bruine AP, Baeten CG. Prognostic role of vasculogenic mimicry in colorectal cancer. Diseases of the colon and rectum. 2009; 52(12):2028-35. doi:10.1007/DCR.0b013e3181beb4ff
67. Potente M, Gerhardt H, Carmeliet P. Basic and therapeutic aspects of angiogenesis. Cell. 2011; 146(6):873-87. doi:10.1016/j.cell.2011.08.039
68. Qiao L, Liang N, Zhang J, Xie J, Liu F, Xu D, et al. Advanced research on vasculogenic mimicry in cancer. Journal of cellular and molecular medicine. 2015; 19(2):315-26. doi:10.1111/jcmm.12496
69. Seftor E, Meltzer P, Kirschmann D, Pe'er J, Maniotis A, Trent J, et al. Molecular determinants of human uveal melanoma invasion and metastasis. Clinical and Experimental Metastasis. 2002; 19(3):233-46.
70. Lezcano C, Kleffel S, Lee N, Larson AR, Zhan Q, DoRosario A, et al. Merkel cell carcinoma expresses vasculogenic mimicry: demonstration in patients and experimental manipulation in xenografts. Lab Invest. 2014; 94(10):1092-102. doi:10.1038/labinvest.2014.99
71. van der Schaft DW, Seftor RE, Seftor EA, Hess AR, Gruman LM, Kirschmann DA, et al. Effects of angiogenesis inhibitors on vascular network formation by human endothelial and melanoma cells. J Natl Cancer Inst. 2004; 96(19):1473-7. doi:10.1093/jnci/djh267
72. Haiaty S, Rashidi MR, Akbarzadeh M, Maroufi NF, Yousefi B, Nouri M. Targeting vasculogenic mimicry by phytochemicals: A potential opportunity for cancer therapy. IUBMB life. 2020; 72(5):825-41. doi:10.1002/iub.2233
73. Oraiopoulou M-E, Couturier D-L, Bunce EV, Cannell IG, Sweeney PW, Naylor H, et al. The in vitro dynamics of pseudo-vascular network formation. Br J Cancer. 2024; 131(3):457-67.
74. Ramos-Vara JA. Technical aspects of immunohistochemistry. Veterinary pathology. 2005; 42(4):405-26.
75. Strober W. Trypan Blue Exclusion Test of Cell Viability. Curr Protoc Immunol. 2015; 111:A3 B 1-A3 B doi:10.1002/0471142735.ima03bs111
76. Vembadi A, Menachery A, Qasaimeh MA. Cell Cytometry: Review and Perspective on Biotechnological Advances. Front Bioeng Biotechnol. 2019; 7:147. doi:10.3389/fbioe.2019.00147
77. Feoktistova M, Geserick P, Leverkus M. Crystal Violet Assay for Determining Viability of Cultured Cells. Cold Spring Harb Protoc. 2016; 2016(4):pdb prot087379. doi:10.1101/pdb.prot087379
78. Joubert A, Marais S, Maritz C. Influence of 2-methoxyestradiol on MCF-7 cells: An improved differential interference contrasting technique and Bcl-2 and Bax protein expression levels. Biocell. 2009; 33(1):67-70.
79. Lampugnani MG. Cell migration into a wounded area in vitro. Methods Mol Biol. 1999; 96:177-82.
80. Yarrow JC, Perlman ZE, Westwood NJ, Mitchison TJ. A high-throughput cell migration assay using scratch wound healing, a comparison of image-based readout methods. BMC biotechnology. 2004; 4:1-9.
81. Grada A, Otero-Vinas M, Prieto-Castrillo F, Obagi Z, Falanga V. Research Techniques Made Simple: Analysis of Collective Cell Migration Using the Wound Healing Assay. J Invest Dermatol. 2017; 137(2):e11-e6. doi:10.1016/j.jid.2016.11.020

82. Ke N, Wang X, Xu X, Abassi YA. The xCELLigence system for real-time and label-free monitoring of cell viability. Mammalian Cell Viability: Methods and Protocols. 2011:33-43.
83. Kho D, MacDonald C, Johnson R, Unsworth CP, O'Carroll SJ, du Mez E, et al. Application of xCELLigence RTCA Biosensor Technology for Revealing the Profile and Window of Drug Responsiveness in Real Time. Biosensors (Basel). 2015; 5(2):199-222. doi:10.3390/bios5020199
84. Atienza JM, Yu N, Kirstein SL, Xi B, Wang X, Xu X, Abassi YA. Dynamic and label-free cell-based assays using the real-time cell electronic sensing system. Assay and drug development technologies. 2006; 4(5):597-607.
85. Bird C, Kirstein S. Real-time, label-free monitoring of cellular invasion and migration with the xCELLigence system. Nature Methods. 2009; 6(8):v-vi. doi:10.1038/nmeth.f.263
86. Kurien BT, Scofield RH. Western blotting. Methods. 2006; 38(4):283-93. doi:10.1016/j.ymeth.2005.11.007
87. Smith PK, Krohn RI, Hermanson GT, Mallia AK, Gartner FH, Provenzano MD, et al. Measurement of protein using bicinchoninic acid. Analytical Biochemistry. 1985; 150(1):76-85. doi:10.1016/0003-2697(85)90442-7
88. Fearnley GW, Odell AF, Latham AM, Mughal NA, Bruns AF, Burgoyne NJ, et al. VEGF-A isoforms differentially regulate ATF-2–dependent VCAM-1 gene expression and endothelial–leukocyte interactions. Molecular biology of the cell. 2014; 25(16):2509-21.
89. Schnegg CI, Yang MH, Ghosh SK, Hsu M-Y. Induction of vasculogenic mimicry overrides VEGF-A silencing and enriches stem-like cancer cells in melanoma. Cancer research. 2015; 75(8):1682-90.
90. El Alaoui-Lasmaili K, Faivre Ba. Antiangiogenic therapy: Markers of response, “normalization” and resistance. Crit Rev Oncol Hematol. 128:118-29. doi:10.1016/j.critrevonc.2018.06.001
91. Jászai J, Schmidt MHH. Trends and Challenges in Tumor Anti-Angiogenic Therapies. Cells. 2019; 8(9) doi:10.3390/cells8091102
92. Vartanian AA, Kosorukov VS. Melanoma Cell Lines as a Basis for Development of a Model of Vasculogenic Mimicry. Biology Bulletin. 2023; 50(3):259-65. doi:10.1134/S1062359023700206
93. Domenico R, Tiziana A, Simona R, Roberto T, Enrico C. Limitations of Anti-Angiogenic Treatment of Tumors. Translational Oncology [Internet]. 2019; 12(7):[981-6 pp.]. Available from: http://dx.doi.org/10.1016/j.tranon.2019.04.022.
94. Frank NY, Schatton T, Kim S, Zhan Q, Wilson BJ, Ma J, et al. VEGFR-1 expressed by malignant melanoma-initiating cells is required for tumor growth. Cancer Res. 2011; 71(4):1474-85. doi:10.1158/0008-5472.CAN-10-1660
95. Graziani G, Ruffini F, Tentori L, Scimeca M, Dorio AS, Atzori MG, et al. Antitumor activity of a novel anti-vascular endothelial growth factor receptor-1 monoclonal antibody that does not interfere with ligand binding. Oncotarget. 2016; 7(45):72868-85. doi:10.18632/oncotarget.12108
96. Rofstad EK, Halsør EF. Vascular endothelial growth factor, interleukin 8, platelet-derived endothelial cell growth factor, and basic fibroblast growth factor promote angiogenesis and metastasis in human melanoma xenografts. Cancer Research. 2000; 60(17):4932-8.
97. Vartanian A, Stepanova E, Grigorieva I, Solomko E, Belkin V, Baryshnikov A, Lichinitser M. Melanoma Vasculogenic Mimicry Capillary-Like Structure Formation Depends on Integrin and Calcium Signaling. Microcirculation. 2011; 18(5):390-9. doi:10.1111/j.1549-8719.2011.00102.x
98. Ding Y-B, Chen G-Y, Xia J-G, Zang X-W, Yang H-Y, Yang L. Association of VCAM-1 overexpression with oncogenesis, tumor angiogenesis and metastasis of gastric carcinoma. World J Gastroenterol. 2003; 9(7):1409.
99. Minn AJ, Gupta GP, Siegel PM, Bos PD, Shu W, Giri DD, et al. Genes that mediate breast cancer metastasis to lung. Nature. 2005; 436(7050):518-24.
100. Siyasi M, Mahjoubi F, Mahjoubi B, Shabani S. Study of VCAM-1 gene expression in normal and tumoral tissues in patients with colorectal cancer. J Biotechnol Biomed. 2017; 1(1):19-26.
101. Shibuya M. Vascular endothelial growth factor and its receptor system: physiological functions in angiogenesis and pathological roles in various diseases. J Biochem. 2012; 153(1):13-9. doi:10.1093/jb/mvs136

102. AboulMagd AM, Abdelwahab NS. Analysis of sunitinib malate, a multi-targeted tyrosine kinase inhibitor: A critical review. Microchemical Journal. 2021; 163 doi:10.1016/j.microc.2021.105926
103. Faivre S, Demetri G, Sargent W, Raymond E. Molecular basis for sunitinib efficacy and future clinical development. Nat Rev Drug Discov. 2007; 6(9):734-45.
104. Mendel DB, Laird AD, Xin X, Louie SG, Christensen JG, Li G, et al. In vivo antitumor activity of SU11248, a novel tyrosine kinase inhibitor targeting vascular endothelial growth factor and platelet-derived growth factor receptors: determination of a pharmacokinetic/pharmacodynamic relationship. Clinical cancer research. 2003; 9(1):327-37.
105. Saraste A, Pulkki K. Morphologic and biochemical hallmarks of apoptosis. Cardiovascular research. 2000; 45(3):528-37.
106. Scholtz W, Mabeta P. Sunitinib malate inhibits hemangioma cell growth and migration by suppressing focal adhesion kinase signaling. J Appl Biomed. 2020; 18(4):143-51. doi:10.32725/jab.2020.019
107. Bravo-Cordero JJ, Hodgson L, Condeelis J. Directed cell invasion and migration during metastasis. Current opinion in cell biology. 2012; 24(2):277-83.
108. Clark. Modes of cancer cell invasion and the role of the microenvironment. Current Opinion in Cell Biology. 2015; 36 doi:info:doi/10.1016/j.ceb.2015.06.004
109. Pasquali S, Hadjinicolaou AV, Sileni VC, Rossi CR, Mocellin S. Systemic treatments for metastatic cutaneous melanoma. Cochrane Database of Systematic Reviews. 2018; (2)
110. Streit M, Detmar M. Angiogenesis, lymphangiogenesis, and melanoma metastasis. Oncogene. 2003; 22(20):3172-9.
111. Hennequin LF, Thomas AP, Johnstone C, Stokes ES, Plé PA, Lohmann J-JM, et al. Design and structure− activity relationship of a new class of potent VEGF receptor tyrosine kinase inhibitors. Journal of medicinal chemistry. 1999; 42(26):5369-89.
112. Ji S, Xin H, Li Y, Su EJ. FMS-like tyrosine kinase 1 (FLT1) is a key regulator of fetoplacental endothelial cell migration and angiogenesis. Placenta. 2018; 70:7-14.
113. Koizumi K, Shintani T, Hayashido Y, Hamada A, Higaki M, Yoshioka Y, et al. VEGF-A promotes the motility of human melanoma cells through the VEGFR1–PI3K/Akt signaling pathway. In Vitro Cell Dev Biol Anim. 2022; 58(8):758-70.
114. Li J, Cui Y, Wang Q, Guo D, Pan X, Wang X, et al. The proliferation of malignant melanoma cells could be inhibited by ranibizumab via antagonizing VEGF through VEGFR1. Molecular Vision. 2014; 20:649.
115. Moravčík R, Stebelová K, Boháč A, Zeman M. Inhibition of VEGF mediated post receptor signalling pathways by recently developed tyrosine kinase inhibitor in comparison with sunitinib. Gen Physiol Biophys. 2016; 35(4):511-4.
116. Andrae N, Kirches E, Hartig R, Haase D, Keilhoff G, Kalinski T, Mawrin C. Sunitinib targets PDGF-receptor and Flt3 and reduces survival and migration of human meningioma cells. European Journal of Cancer. 2012; 48(12):1831-41.
117. Mehnert JM, McCarthy MM, Jilaveanu L, Flaherty KT, Aziz S, Camp RL, et al. Quantitative expression of VEGF, VEGF-R1, VEGF-R2, and VEGF-R3 in melanoma tissue microarrays. Human Pathology. 2010; 41(3):375-84. doi:10.1016/j.humpath.2009.08.016
118. Ruffini F, Failla CM, Orecchia A, Bani MR, Dorio AS, Fortes C, et al. Expression of the soluble vascular endothelial growth factor receptor-1 in cutaneous melanoma: role in tumour progression. British Journal of Dermatology. 2011; 164(5):1061-70. doi:10.1111/j.1365-2133.2010.10200.x
119. Jayasinghe C, Simiantonaki N, Michel-Schmidt R, Kirkpatrick CJ. Comparative study of human colonic tumor-derived endothelial cells (HCTEC) and normal colonic microvascular endothelial cells (HCMEC): Hypoxia-induced sVEGFR-1 and sVEGFR-2 levels. Oncology reports. 2009; 21(4):933-9.
120. Kusmartsev S, Eruslanov E, Kubler H, Tseng T, Sakai Y, Su Z, et al. Oxidative stress regulates expression of VEGFR1 in myeloid cells: link to tumor-induced immune suppression in renal cell carcinoma. J Immunol. 2008; 181(1):346-53.

Appendix I: MSc Committee Approval Letter

UNIVERSITEIT VAN PRETORIA
UNIVERSITY OF PRETORIA
YUNIBESITHI YA PRETORIA

MSc Committee
School of Medicine
Faculty of Health Sciences

01 October 2020

Dr Peace Mabeta
Department of Physiology
Faculty of Health Sciences

Dear Dr,

Mr RB Matlala, Student no 10199544

Please receive the following comments with reference to the MSc Committee submission of the abovementioned student:

Student name	Mr Rakolote Bruce Matlala	**Student number**	10199544
Name of study leader	Dr Peace Mabeta		
Department	Human Physiology		
Title of MSc	Investigation of vasculogenic mimicry in melanoma tissue		
Date of first submission	August 2020		

MSc Committee, School of Medicine
Faculty of Health Sciences
University of Pretoria,
Private Bag X323
Pretoria 0001, South Africa
Tel +27 (0)12 319 2325
Fax +27 (0)12 323 0732

Fakulteit Gesondheidswetenskappe
Lefapha la Disaense tša Maphelo

Comments to study leader August 2020	• Please correct the cell culture in the methodology and state that you will be receiving fixed specimens. • Include the manufacturer's detail of all instruments and reagents used. • Please include for each method the results expected, how the results will be interpreted, and how the results will be captured and stored. • Different stages of melanoma will be studied – please indicate how the data will be analysed. • Please expand the methodology section. Please include detail for each method. • PCR: Please include the expected product sizes. • Please correct the real-time PCR analysis section; normally a reference gene will be used to compare the expression against. • Use numbered headings throughout your protocol. • Please revise the budget to show a true reflection of the number of samples that you will be working on. Please update and include an estimate for all research procedures. • Revise the study design section. The details you placed under study design is study procedure. • Update the timeline. • Include a data capturing sheet. • Revise the reference list; correct all inconsistencies. • Include in the ethics section more detail. Expand on how patient confidentiality and anonymity will be protected. • Please include a description in the data management section how the candidate will comply with the new UP research data management policy. All metadata and final data should be uploaded on the UP research data management system.
September 2020	• Thank you for submitting the revised protocol.
Decision	This protocol has been provisionally approved. Please submit the revised protocol to ethics, and supply the MSc committee with proof of acceptance. The internal and external examiners can be nominated and submitted to the MSc Committee six months prior to submission of the dissertation. Please ensure that the CV of the examiners includes: supervision, examination and publication records.

Yours sincerely

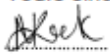

Prof Marleen Kock
Chair: MSc Committee

Appendix II: Ethics Approval Letter

UNIVERSITEIT VAN PRETORIA
UNIVERSITY OF PRETORIA
YUNIBESITHI YA PRETORIA

Faculty of Health Sciences

Institution: The Research Ethics Committee, Faculty Health Sciences, University of Pretoria complies with ICH-GCP guidelines and has US Federal wide Assurance.
- FWA 00002567, Approved dd 18 March 2022 and Expires 18 March 2027.
- IORG #: IORG0001762 OMB No. 0990-0279 Approved for use through June 30, 2025 and Expires 07/28/2026.

Faculty of Health Sciences **Research Ethics Committee**

12 September 2024

Approval Certificate
Annual Renewal

Dear Mr RB Matlala,

Ethics Reference No.: 655/2020 – Line 4
Title: Investigation of vasculogenic mimicry in melanoma tissue

The **Annual Renewal** as supported by documents received between 2024-08-19 and 2024-09-11 for your research, was approved by the Faculty of Health Sciences Research Ethics Committee on 2024-09-11 as resolved by its quorate meeting.

Please note the following about your ethics approval:

- Renewal of ethics approval is valid for 1 year, subsequent annual renewal will become due on 2025-09-12.
- The Research Ethics Committee (REC) must monitor your research continuously. To this end, you must submit as may be applicable for your kind of research:
  a) annual reports;
  b) reports requested *ad hoc* by the REC;
  c) all visitation and audit reports by a regulatory body (e.g. the HPCSA, FDA, SAHPRA) within 10 days of receiving one;
  d) all routine monitoring reports compiled by the Clinical Research Associate or Site Manager within 10 days of receiving one.
- The REC may select your research study for an audit or a site visitation by the REC.
- The REC may require that you make amendments and take corrective actions.
- The REC may suspend or withdraw approval.
- Please remember to use your protocol number (655/2020) on any documents or correspondence with the Research Ethics Committee regarding your research.

Ethics approval is subject to the following:

- The ethics approval is conditional on the research being conducted as stipulated by the details of all documents submitted to the Committee. In the event that a further need arises to change who the investigators are, the methods or any other aspect, such changes must be submitted as an Amendment for approval by the Committee.

We wish you the best with your research.

Yours sincerely

On behalf of the FHS REC, Dr R Sommers
MBChB, MMed (Int), MPharmMed, PhD
Deputy Chairperson *of the Faculty of Health Sciences Research Ethics Committee, University of Pretoria*

The Faculty of Health Sciences Research Ethics Committee complies with the SA National Act 61 of 2003 as it pertains to health research and the United States Code of Federal Regulations Title 46 and 46. This committee abides by the ethical norms and principles for research, established by the Declaration of Helsinki, the South African Medical Research Council Guidelines as well as the Guidelines for Ethical Research: Principles Structures and Processes, Second Edition 2016 (Department of Health).

Research Ethics Committee
Room 4-60, Level 4, Tswelopele Building
University of Pretoria, Private Bag X323
Gezina 0031, South Africa
Tel +27 (0)12 356 3084
E-mail: deepeka.behari@up.ac.za
www.up.ac.za

Fakulteit Gesondheidswetenskappe
Lefapha la Disaense tša Maphelo

Appendix III: Turnitin Report

Turn it in Copy RB Matlala MSc Dissertation Revised_06012025 CLEAN.docx

ORIGINALITY REPORT

11%	9%	12%	0%
SIMILARITY INDEX	INTERNET SOURCES	PUBLICATIONS	STUDENT PAPERS

PRIMARY SOURCES

1	repository.up.ac.za Internet Source	3%
2	Sekoba, Nare Pretty. "Effects of Vascular Endothelial Growth Factor Receptor-1 Inhibition on Vasculogenic Mimicry and the Metabolic Profile of Breast Cancer Cells in Vitro", University of Pretoria (South Africa), 2023 Publication	2%
3	hdl.handle.net Internet Source	1%
4	van Tonder, Alet. "Exploiting Drug Synergism to Extend the Application of Oestrone Analogues", University of Pretoria (South Africa), 2023 Publication	1%
5	www.ncbi.nlm.nih.gov Internet Source	1%
6	"Cutaneous Melanoma", Springer Science and Business Media LLC, 2020 Publication	1%
7	Lai-Cheong, J.E.. "Structure and function of skin, hair and nails", Medicine, 200905 Publication	1%
8	pericles.pericles-prod.literatumonline.com Internet Source	1%
9	mdpi.com Internet Source	1%
10	www.science.gov Internet Source	1%
11	link.springer.com Internet Source	1%